Effect of DPP4/CD26 expression on SARS-CoV-2 susceptibility, immune response, adenosine (derivatives m^6_2A and CD) regulations on patients with cancer and healthy individuals

JIAMAN DU[1*], JIEWEN FU[1*], WENQIAN ZHANG[1], LIANMEI ZHANG[1,2], HANCHUN CHEN[3], JINGLIANG CHENG[1], TAO HE[1,4] and JUNJIANG FU[1]

[1]Key Laboratory of Epigenetics and Oncology, The Research Center for Preclinical Medicine, Southwest Medical University, Luzhou, Sichuan 646000; [2]Department of Pathology, The Affiliated Huaian No. 1 People's Hospital of Nanjing Medical University, Huai'an, Jiangsu 223300; [3]Department of Biochemistry and Molecular Biology, School of Life Sciences, Central South University, Changsha, Hunan 410013; [4]Institute for Cancer Medicine and Basic Medical School, Southwest Medical University, Luzhou, Sichuan 646000, P.R. China

Received September 21, 2022; Accepted January 25, 2023

DOI: 10.3892/ijo.2023.5489

Abstract. The worldwide COVID-19 pandemic was brought on by a new coronavirus (SARS Cov-2). A marker/receptor called Dipeptidyl peptidase 4/CD26(DPP4/CD26) may be crucial in determining susceptibility to tumors and coronaviruses. However, the regulation of DPP4 in COVID-invaded cancer patients and its role on small molecule compounds remain unclear. The present study used the Human Protein Atlas, Monaco, and Schmiedel databases to analyze the expression of DPP4 in human tissues and immune cells. The association between DPP4 expression and survival in various tumor tissues was compared using GEPIA 2. The DNMIVD database was used to analyze the correlation between DPP4 expression and promoter methylation in various tumors. On the cBioPortal network, the frequency of *DPP4* DNA mutations in various cancers was analyzed. The correlation between DPP4 expression and immunomodulators was analyzed by TISIDB database. The inhibitory effects of cordycepin (CD), N6, N6-dimethyladenosine (m^6_2A) and adenosine (AD) on DPP4 in cancer cells were evaluated. DPP4 was mainly expressed in endocrine tissue, followed by gastrointestinal tract, female tissue (mainly in placenta), male tissue (mainly in prostate and seminal vesicle), proximal digestive tract, kidney, bladder, liver, gallbladder and respiratory system. In immune cells, DPP4 mRNA was mainly expressed in T cells, and its expression was upregulated in esophageal carcinoma, kidney renal papillary cell carcinoma (KIRP), liver hepatocellular carcinoma (LIHC), lung adenocarcinoma, pancreatic adenocarcinoma, prostate adenocarcinoma, stomach adenocarcinoma, thyroid carcinoma and thymoma. However, it was downregulated in breast invasive carcinoma, kidney chromophobe, lung squamous cell carcinoma and skin cutaneous melanoma. Thus, DPP4 is involved in viral invasion in most types of cancer. The expression of DPP4 could be inhibited by CD, m^6_2A and AD in different tumor cells. Moreover, CD significantly inhibited the formation of GFP-positive syncytial cells. *In vivo* experiments with AD injection further showed that AD significantly inhibited lymphocyte activating factor 3 expression. These drugs may have potential to treat COVID-19 by targeting DPP4. Thus, DPP4 may be medically significant for SARS-CoV-2-infected cancer patients, providing prospective novel targets and concepts for the creation of drugs against COVID-19.

Correspondence to: Professor Junjiang Fu or Professor Tao He, Key Laboratory of Epigenetics and Oncology, The Research Center for Preclinical Medicine, Southwest Medical University, 3-319 Zhongshan Road, Luzhou, Sichuan 646000, P.R. China
E-mail: fujunjiang@swmu.edu.cn
E-mail: hetao198@swmu.edu.cn

*Contributed equally

Key words: DPP4/CD26 gene, COVID-19, susceptibility, cancers, immune, cordycepin, N6-dimethyladenosine (m^6_2A), adenosine

Introduction

Dipeptidyl peptidase 4 (DPP4; OMIM: 102720), also named CD26, intestinal adenosine deaminase complexing protein 2 (ADCP2), is a type II transmembrane glycoprotein (1-3). One of the lymphocyte membrane-bound proteins, DPP4 possesses serine protease activity. DPP4 is located on human chromosome 2q24.2 and encodes a protein composed of 766 amino acids with a predicted molecular weight of 88,279 Da (4). DPP4 is ubiquitously expressed in different cells, organs and body fluids. It participates in diverse physiological and pathological processes by mediating glucose metabolism (5,6), the endocrine and cardiovascular systems, cell adhesion, apoptosis, fibrosis, inflammation and immune function (1,2,7). These effects are achieved by forming homodimers for

the enzymatic activity and/or protein-protein interactions. For example, DPP4 may interact with the S1 domain of the S-protein (spike glycoprotein) in severe acute respiratory syndrome coronavirus 2 (SARS-CoV-2) to cause coronavirus disease 19 (COVID-19) disease (8). Its binding to caveolin-1 and card-maguk protein 1 induces T-cell proliferation and NF-κB activation (9). Its interaction with adenosine deaminase (ADA) mediates epithelial and lymphocyte cell adhesion (10). Thus, DPP4 plays an important role in the development of immune-mediated disorders (7) and as a receptor of ADA in lymphocytes. Furthermore, it has been shown that DPP4 promotes metastases of types of cancer (11).

In 2003, Conarello *et al* (6) concluded that DPP4 inhibition is a viable therapeutic option for the treatment of metabolic diseases related to diabetes and obesity. DPP4 inhibitors, including hypoglycemic agents (e.g., sitagliptin, alogliptin and linagliptin), have been approved by the U.S. Food and Drug Administration (FDA) for the treatment of type 2 diabetes mellitus (12,13). In addition, clinical trials and preclinical studies have evaluated the efficacy and safety of DPP4 inhibitors in immune-mediated disorders and anti-cancer immune responses (14). It is thought that these inhibitors may act by regulating the balance of the T helper 1/2 (Th1/Th2) phenotype and production of cytokines (15,16). Over-expression of DPP4 in lung diseases may increase the susceptibility to viral invasion. Further evidence showed the role of DPP4 in the pathogenesis of lung disorders, including lung cancer; thus, DPP4 may be a therapeutic target in this setting (12).

DPP4 affects viral attacks in infectious respiratory disorders, including Middle East respiratory syndrome (MERS) (17,18) and non-infectious lung disorders, including lung cancer (19), chronic obstructive pulmonary disorder, pulmonary fibrosis and asthma (20,21). It has been shown that ADA competitively binds to DPP4, thereby preventing the binding of DPP4 with the MERS-CoV S1 domain. Thus, it is a potential agent for blocking viral attacks (22). During the COVID-19 pandemic, it was also shown that DPP4 is a vital marker/receptor that might play a significant role in disease progression (23,24) and susceptibility to COVID-19 (25). Decreased circulating DPP4 activity or expression is prognostic for severe outcomes of COVID-19 (23,26). High DPP4 levels and other receptors (such as CD147 and TMPRSS2) are correlated with the occurrence and severity of COVID-19 (27). Acute respiratory distress syndrome is a leading cause of mortality in patients with COVID-19. DPP4 inhibitors may be a novel therapeutic approach by decreasing the production of inflammatory factors, such as IL-6, IL-1β and TNF-α (28). Studies have documented a potential therapeutic effect of DPP4 inhibitors in patients with diabetes diagnosed with COVID-19 by reducing cytokine production (29-31). DPP4 inhibitors may reduce the mortality rate and improve outcomes of COVID-19 patients with or without type1 and type2 diabetes mellitus (32-37). Clinical trials of DPP4 inhibitors for COVID-19 are currently being performed (38). Several inhibitors of DPP4, such as alogliptin, linagliptin, sitagliptin, saxagliptin and vildagliptin, have been approved worldwide, including by the European Medicines Agency and the U.S. FDA (39). A new monoclonal antibody interacting with angiotensin converting enzyme 2 (ACE2) and DPP4 was recently developed; however, its use in patients has yet to be assessed (40).

Evidence indicates the effects of COVID-19 on the clinical outcome for patients with cancer; patients with cancer and plus COVID-19 are at a high risk of mortality (41-44). Therefore, patients with malignant cancer should be cautious during the COVID-19 pandemic. The correlation between DPP4 and malignancy is currently debatable and its role as a tumor suppressor or promoter of carcinogenesis needs to be determined. Moreover, the mechanisms underlying these processes are complex and warrant further clarification (45).

The present study conducted comprehensive and integrative analyses of DPP4 expression in healthy individuals and patients in the pan-cancer setting using genomic, transcriptomic and epigenomic data. The relationship between the expression of DPP4 and immune cell infiltration was analyzed. The results of analyses may reveal the susceptibility of different types of cancer to SARS-CoV-2 attack and the importance of AD/C-X-C motif chemokine ligand 3 (AD/CXCL3) signaling. By using N6, N6-dimethyladenosine ($m^6{}_2A$), cordycepin (CD) and adenosine (AD) small molecules derived from natural products, the present study may also identify potential therapeutic agents for SARS-CoV-2.

Materials and methods

Online databases. In GenBank, DPP4 in humans is coded as follows: NP_001926.2 for protein and NM_001935.4 for the gene (https://www.ncbi.nlm.nih.gov/protein/NP_001926.2; https://www.ncbi.nlm.nih.gov/nuccore/NM_001935.4?report=genbank&log$=seqview) (46,47). Analysis of DPP4 expression in healthy and cancer tissues was performed using data from the Human Protein Atlas (HPA) (https://www.proteinatlas.org/ENSG00000197635-DPP4/tissue) (48,49). The *DPP4* expression in different cancer tissues and matched healthy tissues, survival, isoforms, distribution and structure of the domain were analyzed through Gene Expression Profiling Interactive Analysis 2 (GEPIA2; http://gepia2.cancer-pku.cn/#analysis) (50,51). DNA methylation analysis of the DPP4 promoter in the pan-cancer setting was performed using the DNA methylation interactive visualization database (DNMIVD) (http://119.3.41.228/dnmivd/query_gene/?cancer=pancancer&gene=DPP4) (52). Mutation analysis for the *DPP4* gene was performed through tumor genomics in cBioPortal (https://www.cbioportal.org/results/cancerTypesSummary?case_set_id=all&gene_list=DPP4&cancer_study_list=5c8a7d55e4b046111fee2296) (53). An integrated repository portal, called tumor-immune system interactions database (TISIDB), was utilized to analyze the relationship between the abundance of tumor-infiltrating lymphocytes (TILs) and DPP4 expression (http://cis.hku.hk/TISIDB/browse.php?gene=DPP4) (54).

Reagents, cell lines and breast cancer tissue collections. CD (cat no. B20196) was purchased from Must Bio-Technology Co. Ltd. AD (cat no. A6218) and $m^6{}_2A$ (cat no. N879945) were purchased from Macklin Biochemical Technology Co., Ltd. Dimethyl sulfoxide (DMSO; cat. no. D8148) was purchased from MilliporeSigma. The total RNA extraction kit (cat no. DP419), buffer RZ solution (cat no. RK145) and 2XTaq PCR Master Mix (cat no. KT211) were purchased from TransGen Biotech Co Ltd. The reverse transcription (RT) PCR kit (cat no. FSQ-201) was purchased from Toyobo Biotech

Co., Ltd. Sodium dodecyl sulfate (SDS; cat. no. L5750) and β-actin antibodies (cat. no. A1978) were purchased from MilliporeSigma. The DPP4 antibody (cat. no. 67138S), mouse (cat. no. 7076S) and rabbit (cat. no. 7074S) secondary antibodies were purchased from Cell Signaling Technology, Inc. The lymphocyte activating 3 (LAG-3) polyclonal antibody (cat no. 16616-1-AP) was purchased from Wuhan Sanying Biotechnology. RPMI 1640 medium (cat no. C3010-0500) and Dulbecco's modified Eagle's medium (DMEM; cat no. C3113-0500) were purchased from Shanghai VivaCell Biosciences, Ltd. Fetal bovine serum (FBS; cat. no. A6907) was purchased from Invigentech. Phosphate buffered saline (PBS; cat no. P1010) was purchased from Beijing Solarbio Science & Technology Co., Ltd. The trypsin-ethylenediaminetetraacetic acid (Trypsin-EDTA) solution (cat no. C0201) and penicillin/streptomycin solution (cat no. C0222) were purchased from Beyotime Institute of Biotechnology. The lung cancer cell lines H1975 and A549, breast cancer cell line BT549 and prostate cancer cell lines PC3 and 22RV1 were purchased from the American Type Culture Collection.

A total of 11 paired of breast cancer tissues and the matched normal tissues from Chinese women were collected with informed consent (the affiliated hospital of Southwest Medical University; the date range was between January 2021 and September 2022). Total proteins were extracted for western blotting. All were invasive breast cancers with patients' age range 40-64. The present study was approved by the Ethical Committee of Southwest Medical University (approval no. 20221117-049).

Animals. All animal experiments were performed in strict accordance with international, national and institutional animal care guidelines. The present study was reviewed and approved by the Ethics Committee of Southwest Medical University, Sichuan, China (approval no. 20221117-049). A total of six BALB/c female mice (20 weeks old, ~24 g) of specific-pathogen-free were purchased from Chongqing Tengxin Biotechnology Co., Ltd. The mice were kept under constant temperature at 22˚C, 50-60% humidity and a 12 h light/dark cycle (lights on from 7 a.m. to 7 p.m.) according to the feeding standard. All mice were healthy and pathogen-free, with free access to diet and water. After AD injection, the mice were observed every 12 h and showed no abnormalities. After 24 h, sodium pentobarbital (200 mg/kg body weight) was injected intraperitoneally to sacrifice the mice. Mortality was defined as no heartbeat following injection and dilated pupils. The whole mouse experiment was conducted for 14 days.

Isolation of mouse lymphocytes. The six BALB/c female mice were divided into the experimental and control groups (three mice per group). AD (0.006 mg/μl) solution (containing 20% DMSO, 30% polyethylene glycol 400, 5% Tween 80 and 63% NaCl) was injected into each mouse in the experimental group through the caudal vein for 24 h. Each mouse in the experimental group received an injection with 25 mg/kg AD. The mice were sacrificed and the spleens were isolated, ground and filtered using 100 μm cell strainers (cat no. 15-1100; Biologix Group Ltd.) in an ice bath. Each sample was collected in a 15 ml tube and centrifuged at 4˚C, 400-600 g, 5 min. The supernatant was collected, sterile 1Xred blood cell lysis solution (150 mmol/l NH_4Cl, 10 mmol/l $KHCO_3$ and 0.1 mmol/l EDTA) (55) was added and the mixture was thoroughly mixed and placed on ice for 5-8 min. Following lysis, the reaction was terminated with sterile cold 1XPBS. The samples were centrifuged at 4˚C, 400-600 g, 15 min, the debris was discarded and the supernatant was mixed with cold 1XPBS. Each sample was divided into two Eppendorf tubes for protein and RNA extraction.

Immunohistochemistry assay (IHC). IHC was performed using formalin-fixed, paraffin-embedded sections of breast and lung cancer tissues obtained from Chinese patients was performed as previously described (47,56-60). DPP4 antibody (1:100 dilution) was used in IHC. Histopathological images were captured using a fluorescence microscope (cat no. DM2500; Leica Microsystems GmbH).

Cell culture. RPMI 1640 medium containing 10% FBS and 1% double antibiotics (penicillin-streptomycin) was used for H1975, A549, PC3 and 22RV1 cells; DMEM containing 10% FBS was used for BT549 and 293T-hACE2 cells (a gift from Professor Xianghui Fu of Sichuan University) (61). When the cell density reached ~50-70% or when the cells entered the logarithmic growth phase 24 h later, CD, AD, or $m^6{}_2A$ were added to the experimental group. Specifically, H1975 and BT549 cells were treated with CD, AD, or $m^6{}_2A$ at different concentrations (0, 10, 20 and 40 μM) for 24 h in a 12-well plate (57). All cells were cultured in an incubator at 37˚C and 5% CO_2.

Cell transfection and syncytia formation. Syncytia formation is a hallmark cellular event in SARS-CoV-2 infection (62). 293T-hACE2 cells were used to transfect the plasmid pCDH-CMV-HnCoV-S-EF1-copGFP. A six-well plate was used as an example, and the cell density was 40-50% for transfection. Lipofectamine® 3000 (cat no. L3000001; Invitrogen; Thermo Fisher Scientific Co., Ltd.) and P3000 were added to each 100 ng of plasmid at 0.3 μl. Then, two EP tubes were prepared in each well, labeled tube 1 and tube 2. Opti-MEM (cat no. 31985070; Thermo Fisher Scientific Co., Ltd.), P3000 and plasmid were added to tube 1, and Opti-MEM and Lipofectamine® 3000 (cat no. L3000001; Invitrogen; Thermo Fisher Scientific Co., Ltd.) were added to tube 2. The two tubes were mixed and left at room temperature for 5 min. After rinsing twice with 1 ml 1XPBS, 1 ml Opti-MEM was added to each well. The mixture of tube 1 and tube 2 was added to the corresponding wells and the mixture was shaken and mixed to make the mixture evenly cover the cells. The cells were placed into a constant temperature incubator at 37˚C and 5% CO_2 saturated humidity for another 6 h. After 6 h, the mixture in the 6-well plate was removed and 2 ml of fresh complete medium was added. Following continued culture for 18 h, the control group was without CD treatment, the experimental group was treated with 20 μM CD for 24 h. The syncytium formation of each group was observed and analyzed using a ZOE Fluorescent Cell Imager (Bio-Rad Laboratories, Inc.). The DPP4 protein and mRNA levels were also measured.

Western blotting. After treatment with CD, AD, or $m^6{}_2A$, the cells were rinsed twice with ice-cold 1XPBS and lysed

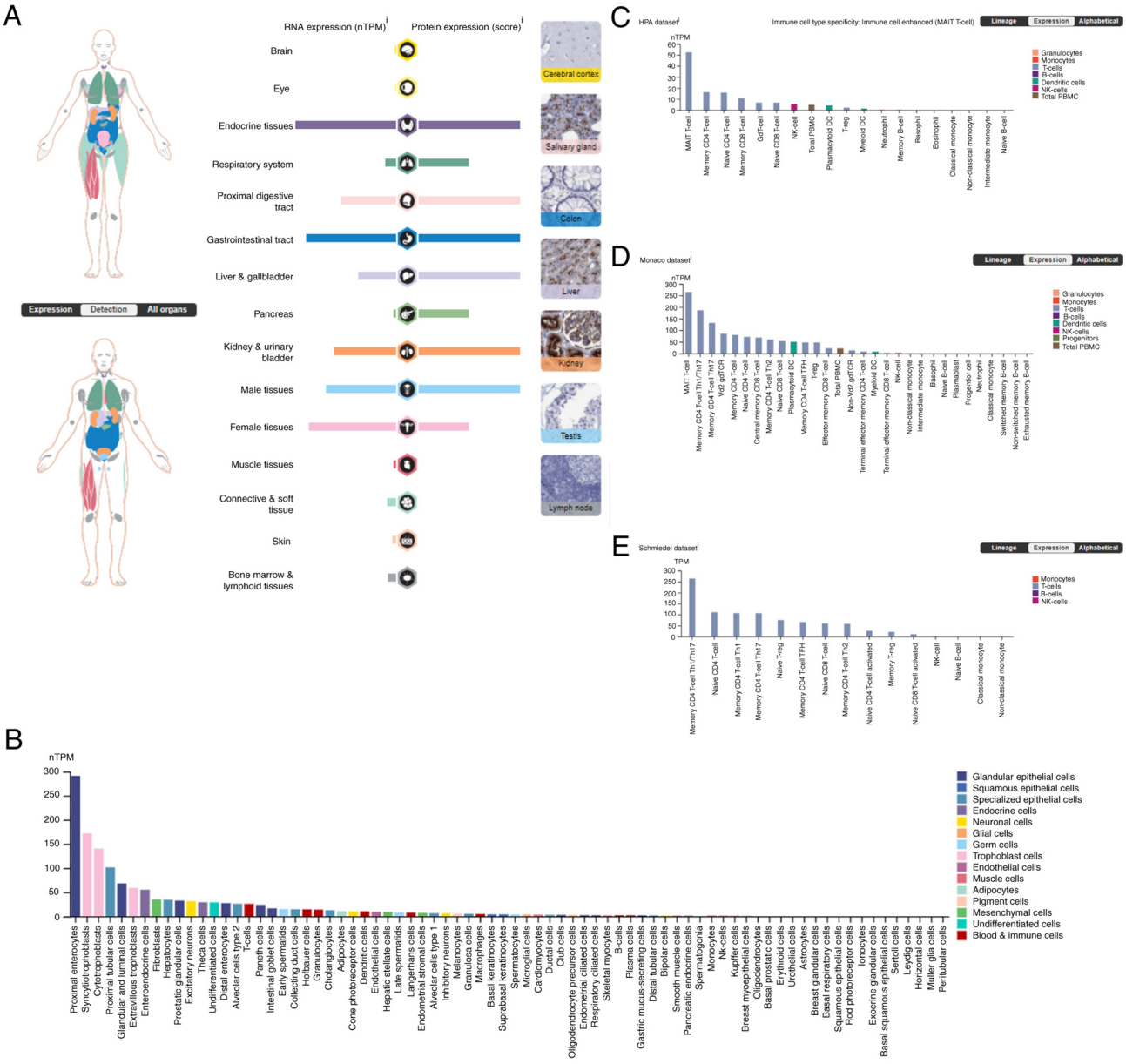

Figure 1. DPP4 expression in human healthy tissues. (A) Summary of mRNA and protein expression. (B) DPP4 mRNA expression for single cell types. (C) DPP4 mRNA expression in immune cell types in the HPA dataset. (D) DPP4 mRNA expression in immune cell types in the Monaco dataset. (E) DPP4 mRNA expression in immune cell types in the Schmiedel dataset. DPP4, dipeptidyl peptidase 4; HPA, Human Protein Atlas; nTPM, normalized transcripts per kilobase per million mapped reads.

using ice-cold 1XEBC buffer (containing 20 mM Tris-HCl pH8.0, 125 mM NaCl, 2 mM EDTA, 0.5% NP-40 and protease inhibitors). Protein concentration was determined using Coomassie brilliant blue staining, diluted to the same concentration. An equal volume of loading buffer (2XSDS) was added to each sample for protein extraction. The samples with the mass of protein ~50 μg per lane were subjected to 10% SDS-polyacrylamide gel electrophoresis. Subsequently, proteins were transferred onto polyvinylidene difluoride membranes. The membranes were blocked with 1XPBST (1XPBS plus 0.05% Tween20) containing 5% skimmed milk for 1-2 h at room temperature, followed by addition of 2% skimmed milk solution. Next, the membranes were incubated with the primary anti-DPP4 antibody (1:2,000 dilution) overnight at 4˚C and washed thrice with 1XPBST. Thereafter, the membranes were incubated with secondary antibody (1:2,000 dilution) at room temperature for 2-4 h on a decolorizing shaker and washed thrice with 1XPBST. Finally, the membranes were soaked in fresh SuperSignal West Pico Chemiluminescence Substrate (cat no. 34580; Thermo Fisher Scientific Inc.) and visualized using a gel imaging system (Bio-Rad Laboratories, Inc.). β-actin served as an internal control. The protocols for western blotting analysis of breast cancer tissues and matched healthy tissues obtained from Chinese patients has been previously described (56,57).

Cycloheximide (CHX) chase assays. Chase assay for DPP4 was performed with 20 μg/ml cycloheximide (CHX; cat no. HY-12320; Med Chem Express Technology Co., Ltd.)

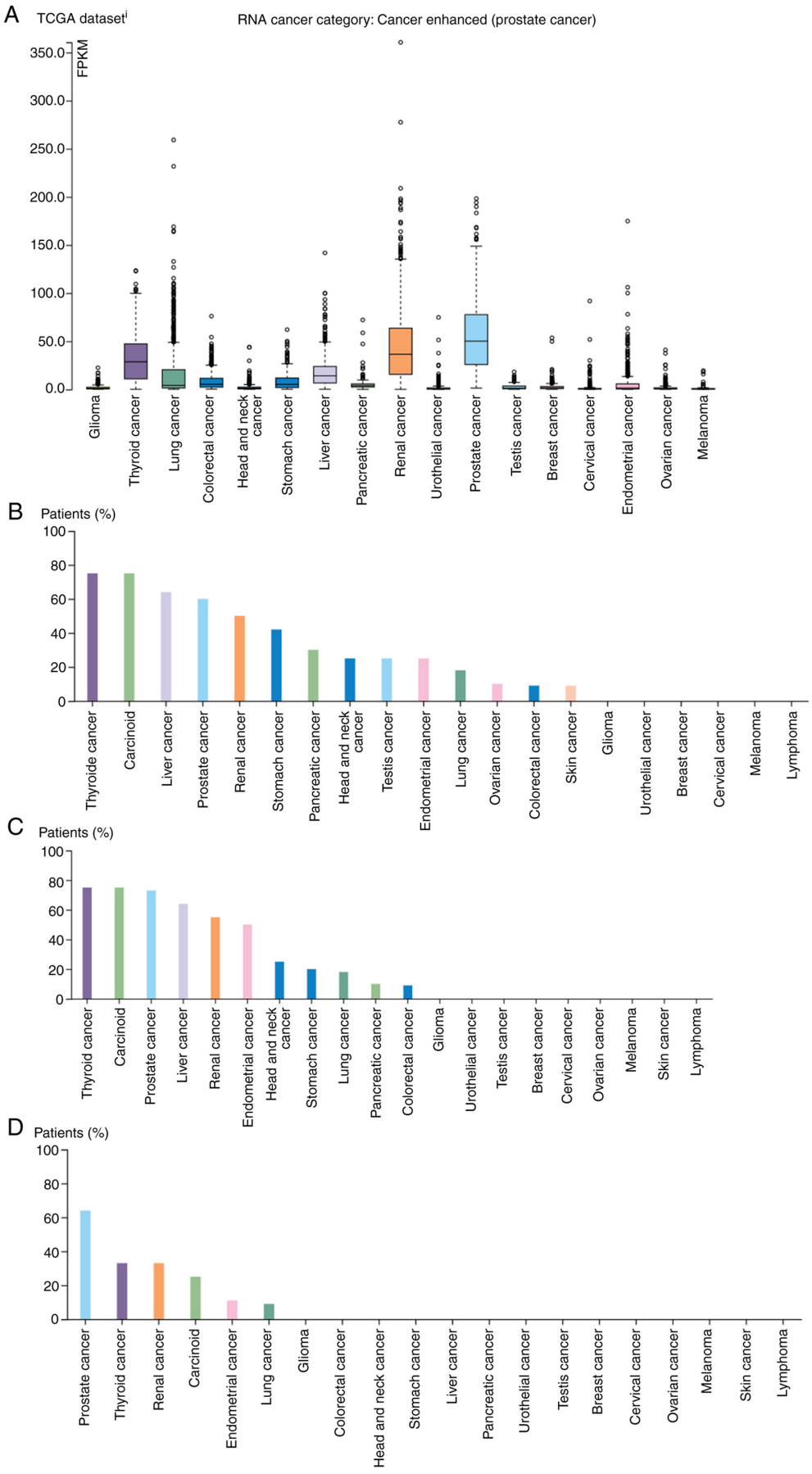

Figure 2. DPP4 expression in human tumor tissues. (A) Overview of DPP4 RNA expression in human tumor tissues. (B) DPP4 protein expression in human tumor tissues, detected using the HPA068778 antibody. (C) DPP4 protein expression in human tumor tissues, detected using the HPA071236 antibody. (D) DPP4 protein expression in human tumor tissues, detected using the CAB045970 antibody. DPP4, dipeptidyl peptidase 4; FPKM, fragments per kilobase per million mapped; HPA, Human Protein Atlas.

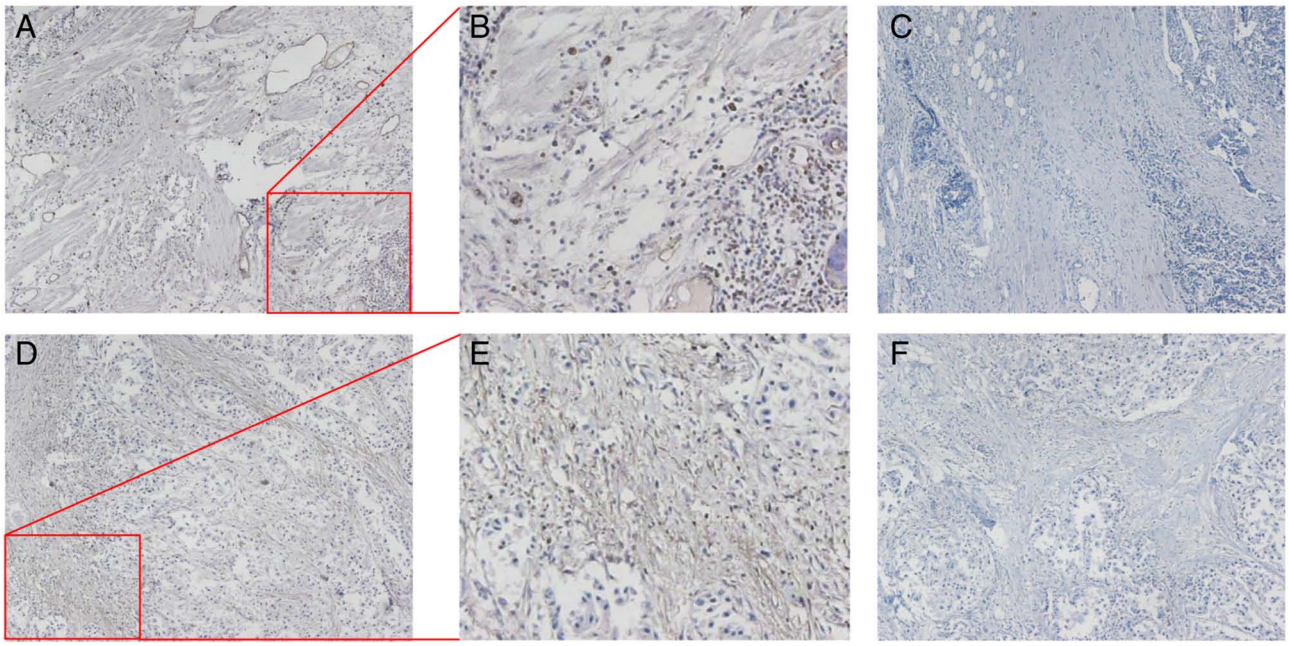

Figure 3. IHC staining for DPP4 expression in human tumor tissues. (A and B) Patients with lung small cell carcinoma. (C) No staining for lung small cell carcinoma. (D and E) Patients with breast cancer. (F) No staining for breast cancer tissue. Magnification, x100. IHC, immunohistochemistry; DPP4, dipeptidyl peptidase 4.

and AD using H1975 cells, as previously described (57). All experiments were performed in triplicate.

RNA extraction and RT. RNA extraction and cDNA synthesis were performed according to the manufacture's protocols. Cell treated with CD, AD, or $m^6{}_2A$ were rinsed twice with ice-cold 1XPBS buffer. Next, buffer RZ solution was added at a concentration of 10 cm^2/ml for 5 min. Subsequently, the cells were lysed using an RNA extraction kit (cat no. DP419; Tiangen Biotech Co., Ltd.). The concentration and purity of the extracted total RNA were determined using a Nanodrop spectrophotometer (Thermo Fisher Scientific Inc.) at an optical density 260/280 nm of=1.8-2.0. RNA integrity evaluated through 1% agarose gel electrophoresis. Thereafter, the extracted RNA was reversely transcribed into cDNA with reverse transcriptase. Total RNA (1 μg) and 5XRT Master Mix (2 μl) were place in a tube and ddH_2O was added to a total volume of 10 μl. The RT reaction was performed as follows: 37˚C for 15 min; 50˚C for 5 min; 98˚C for 5 min; and maintenance at 4˚C until use.

Semi-quantitative PCR. Each PCR tube (total volume: 10 μl) was placed in an ice bath and contained the following: 2XTaq PCR Master MIX (5 μl); primers (1 μl), cDNA (1 μl); and ddH_2O (3 μl). Following thorough mixing and centrifugation, PCR was performed as follows: pre-denaturation at 95˚C for 90 sec; denaturation at 95˚C for 30 sec, annealing at 60˚C for 30 sec, extension at 72˚C for 30 sec; 32 cycles for *DPP4* and 23 cycles for β actin (*ACTB)*, final extension at 72˚C for 5 min and maintenance at 16˚C until use (63). The *DPP4* primers used in semi-quantitative RT-PCR were RT-DPP4-L: 5'-caaattgaagcagccagaca-3' and RT-DPP4-R: 5'-cagggctttg-gagatctgag-3'. The size of the PCR product for DPP4 was 354bp. The *Lag-3* primers in mouse for semi-quantitative RT-PCR included RT-mLag-3-L: 5'-gccatctcgttctcgttctc-3' and RT-mLag-3-R: 5'-tttttgatgctgctgacagg-3'. PCR product size was 335 bp for Lag-3. Of note, Actb served as an internal control. The Actb primers in mouse for semi-quantitative RT-PCR included RT-*ACTB*-mL: 5'-TGTTACCAACTG GGACGACA-3' and RT-*ACTB*-mR: 5'-TCTCAGCTGTGG TGGTGAAG-3'. PCR product size was 392 bp for Actb. The *ACTB* primers in human semi-quantitative RT-PCR included RT-*ACTB*-5: 5'-CTCTTCCAGCCTTCCTTCCT-3' and RT-*ACTB*-3: 5'-CACCTTCACCGTTCCAGTTT-3'. The expected product size was 510 bp. By using the nucleic acid dye GoldView (cat no. G8142; Beijing Solarbio Science & Technology Co., Ltd.), PCR products were verified with 1.5% agarose gel electrophoresis. PCR assays were performed in triplicate.

Statistical analysis. Clinical data from The Cancer Genome Atlas (TCGA) database (64) for cancers were used for overall survival (OS) analysis. The two group of patients according to the upper quartile expression of DPP4 were compared using Kaplan-Meier survival curves (https://kmplot.com/analysis/index.php?p=service). Experimental statistical analysis was performed for six values using independent samples t-test (two groups) for mouse experiments and calculated P-values, expressed as mean ± standard deviation. The mean grayscale values and fluorescence area of individual fluorescence images were measured using ImageJ software (National Institutes of Health). Spearman and Pearson were used to analyze the correlations between gene expression levels and promoter methylation levels in different tissues. All statistical analyses were performed using SPSS version 13.0 (SPSS, Inc.) and GraphPad Prism8 (Dotmatics) software. $P<0.05$ was considered to indicate a statistically significant difference.

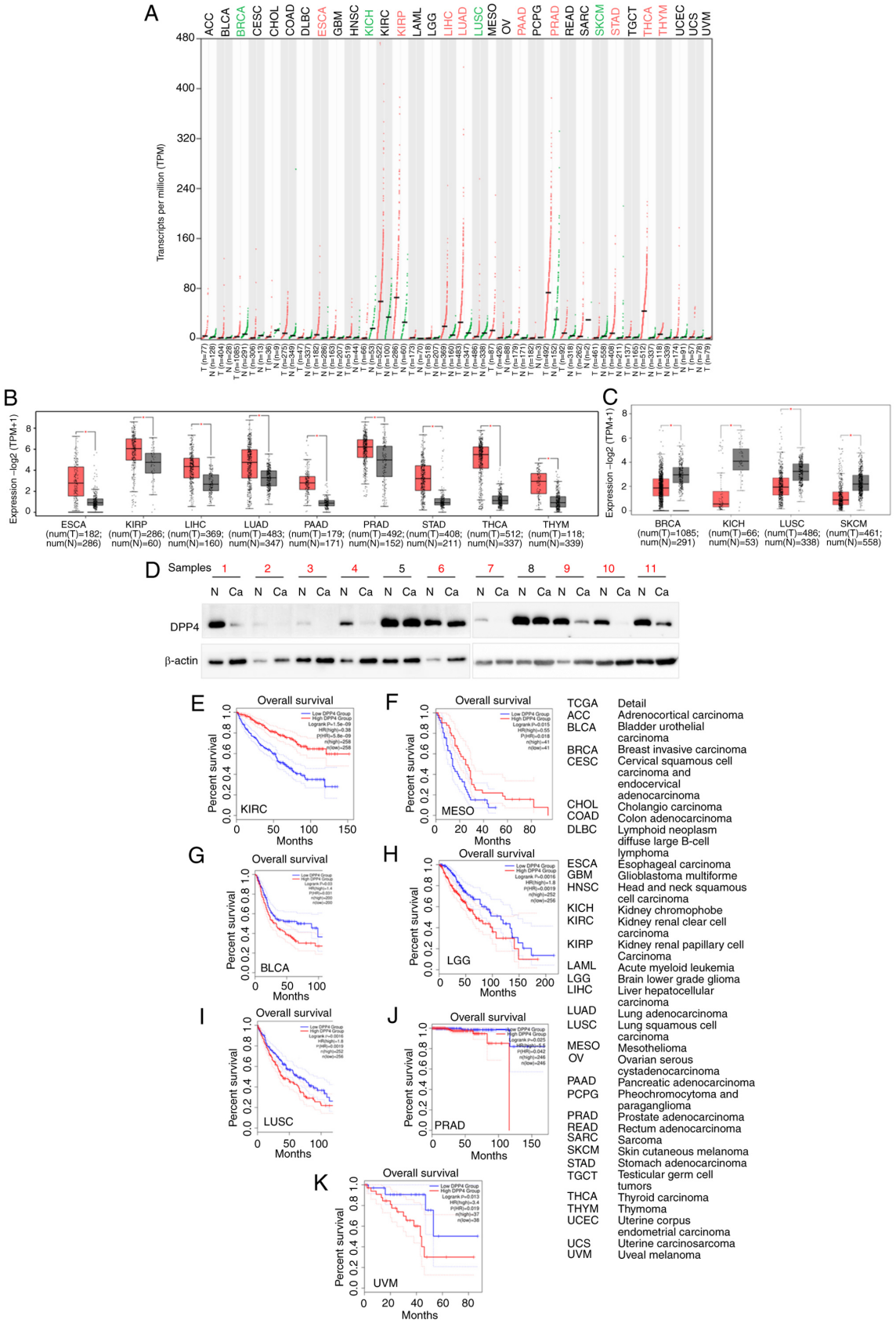

Figure 4. Comparison of DPP4 expression between human tumor tissues and corresponding healthy tissues. (A) comparison of the DPP4 expression profiles in different types of human tumor tissues and corresponding healthy tissues. (B) Box plots showing that DPP4 expression is increased in different types of human tumor tissues compared with matched healthy tissues. (C) Box plots showing that DPP4 expression is decreased in different types of human tumor tissues compared with matched healthy tissues. (D) Validation of the upregulation of DPP4 in breast cancer tissues through western blotting. Overall survival analysis based on the DPP4 expression and Kaplan-Meier curves for (E) KIRC, (F) MESO, (G) BLCA, (H) LGG, (I) LUSC, (J) PRAD and (K) UVM, respectively. The right panel provides the full description of all types of cancer. The log rank P-value ≤0.5 was set as a difference and log rank P-value ≤0.01 was set as a significant difference. DPP4, dipeptidyl peptidase 4; KIRC, kidney renal clear cell carcinoma; MESO, mesothelioma; BLCA, bladder urothelial carcinoma; LGG, brain lower grade glioma; LUSC, lung squamous cell carcinoma; PRAD, prostate adenocarcinoma; UVM, uveal melanoma; HR, hazard ratio.

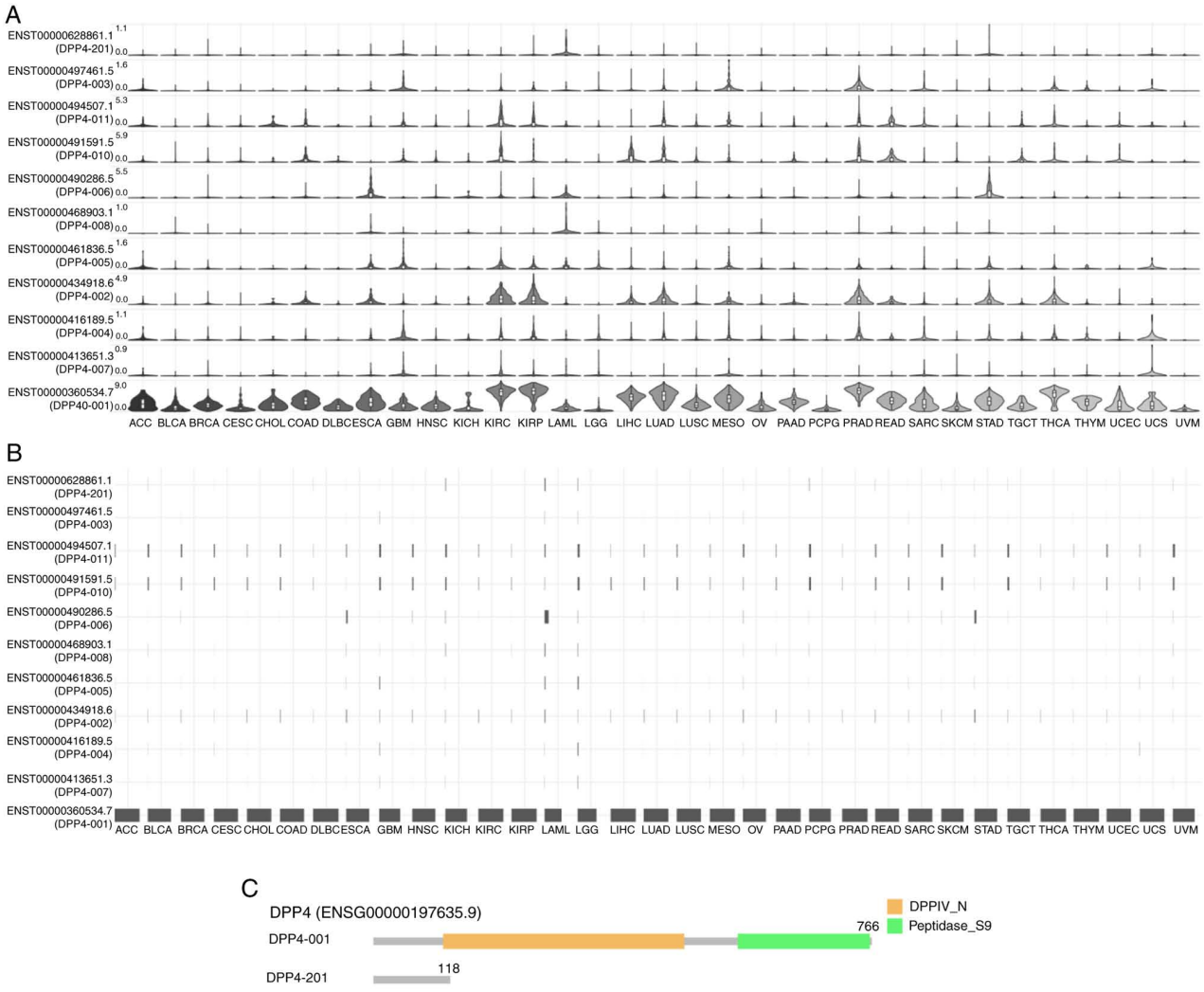

Figure 5. Distribution profiles of DPP4 expression in (A) violin plots and (B) isoform usage in bar plots in multiple types of cancer. (C) DPP4 structure in multiple types of cancer. Note: Information on nine isoforms is missing, including ENST00000413651.3, ENST00000416189.5, ENST00000434918.6, ENST00000461836.5, ENST00000468903.1, ENST00000490286.5, ENST00000491591.5, ENST00000494507.1 and ENST00000497461.5. The full names of types of cancer are shown in Fig. 4. DPP4, dipeptidyl peptidase 4.

Results

DPP4 expression in human healthy tissues. *DPP4* mRNA expression is expressed in endocrine tissues, the gastrointestinal tract, female tissue (mainly in placenta), male tissue (mainly in prostate and seminal vesicle), proximal digestive tract, kidneys, bladder, liver, gallbladder and the respiratory system (Fig. 1A). DPP4 protein is expressed endocrine tissues, the gastrointestinal tract, female tissue (mainly in placenta), male tissue (mainly in prostate and seminal vesicle), proximal digestive tract, kidneys, bladder, liver, gallbladder, the respiratory system and the pancreas (Fig. 1A). Although the *DPP4* mRNA levels were low [lung, 16.0 normalized transcripts per kilobase per million mapped reads (nTPM)], moderate expression of DPP4 protein was observed (Fig. 1A), demonstrating the role of DPP4 in viral invasion in the lungs/bronchus/nasopharynx. *DPP4* mRNA levels were high in various cell types, including proximal enterocytes (glandular epithelial cells, 291.1 nTPM), syncytiotrophoblasts (trophoblast cells, 172.0 nTPM), cytotrophoblasts (trophoblast cells, 140.3 nTPM) and proximal tubular cells (squamous epithelial cells, 101.4 nTPM) (Fig. 1B).

The mRNA expression of *DPP4* in immune cells was analyzed and three datasets are presented (Fig. 1C-E). In the HPA dataset, which includes 18 immune cell types and total peripheral blood mononuclear cells (PBMC), the results showed that *DPP4* mRNA is mainly expressed in T cells [mucosal associated invariant T (MAIT) cells, 53.3 nPTM), natural killer cells (5.3 nPTM) and total PBMC (4.7 nPTM; Fig. 1C)]. In the Monaco dataset, which includes 29 immune cell types and total PBMC, the results indicated that *DPP4* mRNA is mainly expressed in T cells (MAIT, 264.4 nPTM, memory CD4 T-cell Th1/Th17, 186.0 nPTM), dendritic cells (50.3 nPTM) and total PBMC (22.3 nPTM) (Fig. 1D). In the Schmiedel dataset, which includes 15 immune cell types, the results indicated that *DPP4* mRNA is mainly expressed in T cells (memory CD4 T-cell Th1/Th17, 263.5 nPTM) (Fig. 1E). Collectively, these data demonstrated that DPP4 is highly expressed in T cells.

DPP4 expression in human tumor tissues from TCGA. The *DPP4* RNA expression was high in tumor tissues, with the highest levels recorded for prostate cancer [50.1 fragments

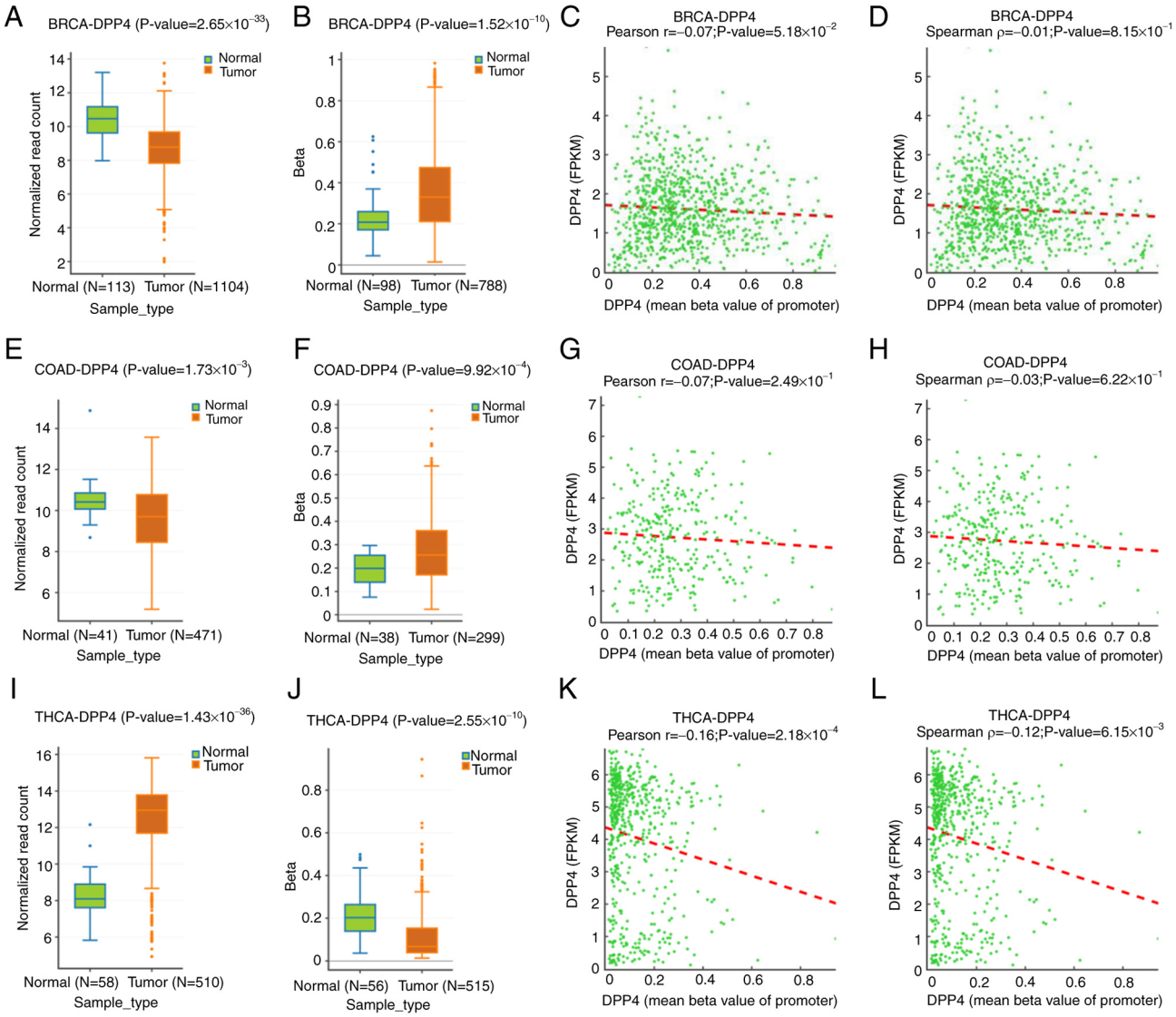

Figure 6. Methylation status of the *DPP4* promoter in tumor tissues and corresponding healthy tissues. (A-D) Expression levels, methylation status at the promoter region, Pearson correlation and Spearman correlation for DPP4 in BRCA tissues and corresponding healthy tissues, respectively. (E-H) Expression levels, methylation status at the promoter region, Pearson correlation and Spearman correlation for DPP4 in COAD tissues and matched healthy tissues, respectively. (I-L) Expression levels, methylation status at the promoter region, Pearson correlation and Spearman correlation for DPP4 in THCA tissues and corresponding healthy tissues, respectively. DPP4, dipeptidyl peptidase 4; BRCA, breast invasive carcinoma; COAD, colon adenocarcinoma; THCA, thyroid carcinoma.

per kilobase per million mapped fragments (FPKM)], renal cancers (36.5 FPKM), including kidney chromophobe (KICH), kidney renal clear cell carcinoma (KIRC) and kidney renal papillary cell carcinoma (KIRP) and thyroid cancer (28.6 FPKM; Fig. 2A).

For protein expression, moderate-to-strong cytoplasmic or membranous positivity for the DPP4 antibody HPA068778 was mainly observed in renal, liver, stomach and prostate tissues; the highest levels were noted in thyroid, carcinoid, liver, prostate, renal and other types of cancer (Fig. 2B). A moderate-to-strong cytoplasmic and membranous positivity for the DPP4 antibody HPA071236 was observed in carcinoid, endometrial, prostate, thyroid, renal and liver tissues; the remaining cancers were essentially negative. The highest levels were observed in thyroid, carcinoid, prostate, liver, renal, endometrial and other types of cancer (Fig. 2C). As shown by the analysis using the DPP4 antibody CAB045970, several cases of prostate cancer and a few cases of renal cell carcinoma presented a moderate-to-strong membranous and/or cytoplasmic positivity, whereas the remaining types of cancer were negative. The highest in prostate cancer, thyroid, renal, carcinoid, endometrial and lung cancer (Fig. 2D). Thus, DPP4 protein is mainly expressed in thyroid, carcinoid, prostate, renal and liver cancer. The present study also conducted IHC using tissues obtained from patients with lung small cell carcinoma and breast cancer. The localization of DPP4 protein in lung small cell carcinoma and breast cancer is shown in Fig. 3. A moderate-to-strong cytoplasmic and membranous positivity was revealed, suggesting the involvement of DPP4 in viral invasion.

DPP4 expression and prognostic value in various tumor tissues and matched healthy tissues. Patients with cancer are vulnerable to SARS-CoV-2 infection and the combination of

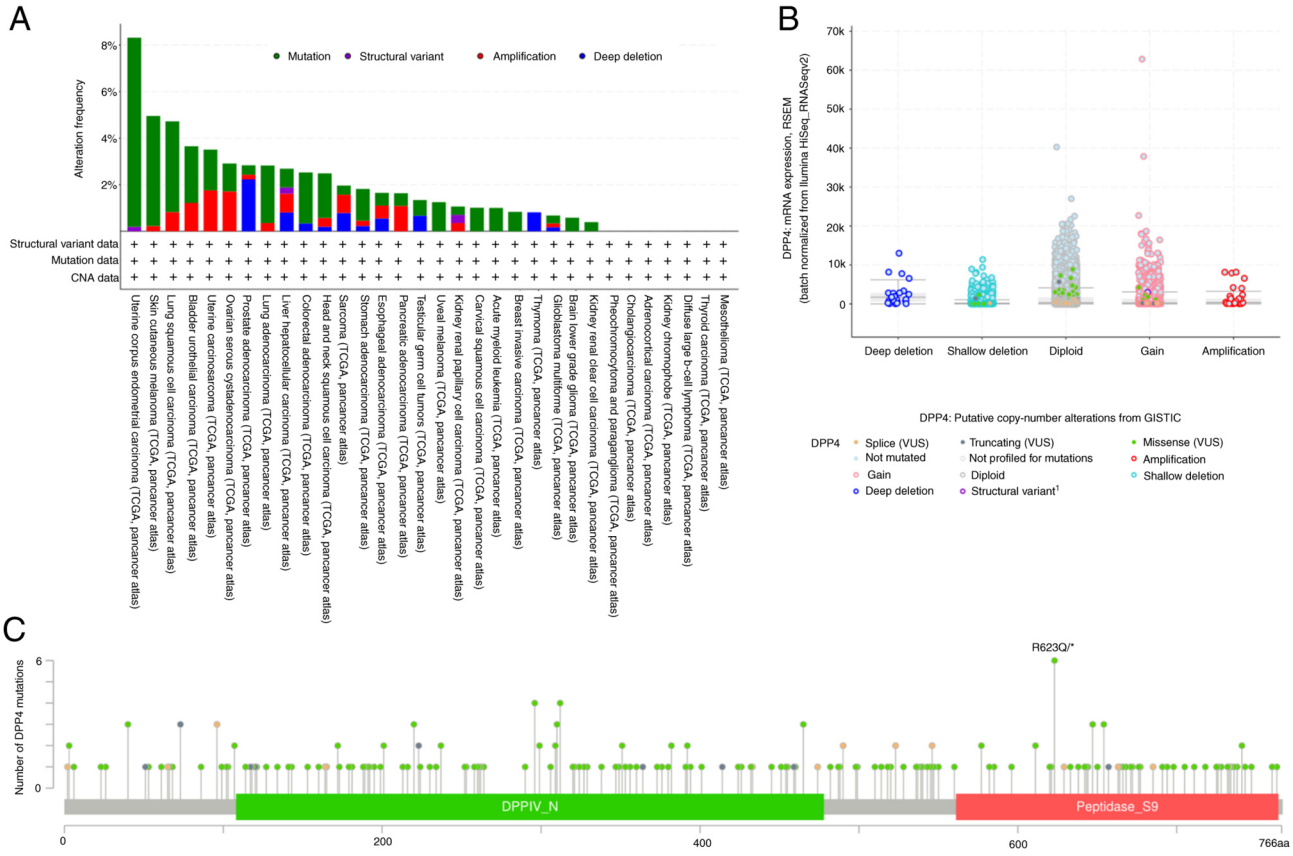

Figure 7. The *DPP4* DNA alterations across different types of cancer. (A) The overview of *DPP4* DNA mutations across different types of cancer. Different colors present different mutation types. (B) *DPP4* mRNA expression vs. its putative copy-number alterations. (C) The hot spots of *DPP4* DNA mutations across different types of cancer. DPP4, dipeptidyl peptidase 4; GISTIC, Genomic Identification of Significant Targets in Cancer.

these conditions is associated with a high mortality rate (41-44). Therefore, it is important to identify differences in the expression levels of DPP4 between tumor tissues of various types of cancer and matched healthy tissues. The results of the GEPIA2 analysis revealed that the levels of *DPP4* are upregulated in esophageal carcinoma (ESCA), KIRP, liver hepatocellular carcinoma (LIHC), lung adenocarcinoma (LUAD), pancreatic adenocarcinoma (PAAD), prostate adenocarcinoma (PRAD), stomach adenocarcinoma (STAD), thyroid carcinoma (THCA) and thymoma (THYM) compared with matched healthy tissues. However, they are downregulated in breast invasive carcinoma (BRCA), KICH, lung squamous cell carcinoma (LUSC) and skin cutaneous melanoma (SKCM; Fig. 4A-C). To verify these data, breast cancer samples with predicted downregulation of DPP4 were collected and western blotting was performed (Fig. 4D). The findings revealed that DPP4 protein levels were decreased in nine of 11 tumor tissues (81.8%) compared with the corresponding healthy tissues. This observation confirmed the results of the mRNA analysis from TCGA database for patients with BRCA.

Further investigation of the prognostic value of *DPP4* demonstrated that higher expression levels were associated with a long OS in KIRC and mesothelioma (MESO) (Fig. 4E-F), implying that DPP4 could be a favorable marker. However, high expression was also linked to a short OS in bladder urothelial carcinoma (BLCA), lower grade glioma (LGG), LUSC, PRAD and UVM (Fig. 4G-K), suggesting that DPP4 could be an unfavorable marker.

DPP4 isoform expression, distribution and structure in different types of cancer. Various isoforms may play different roles in host susceptibility to SARS-CoV-2 invasion (65,66). Thus, analysis of the prevalence and structures of DPP4 isoforms in the pan-cancer setting was performed. According to the results, 11 isoforms exhibited different DPP4 expression levels (Fig. 5A). The expression of isoform ENST00000360534.7(DPP4-001) was high in all 33 types of cancer; nevertheless, the expression of other isoforms was very low or no detectable (Fig. 5A). Identical results were obtained regarding the utilization of isoforms (Fig. 5B). The genomic structures of DPP4 isoforms in 33 types of cancer are shown in Fig. 5C. The isoform DPP4-001 has 766 amino acids and includes the DPPIV_N domain and Peptidase_S9 domain. However, the DPP4-201 isoform has 118 amino acids and lacks functional domains. Information on the other nine isoforms is missing. These results indicated that ENST00000360534.7(DPP4-001) may be the functional isoform for tumorigenesis and SARS-CoV-2 entry in patients in the pan-cancer setting.

DNA methylation of the DPP4 promoter region may regulate DPP4 expression in some types of cancer. DNA methylation could be a mechanism underlying the regulation of DPP4 gene expression. Thus, the present study investigated the types of cancer in which DPP4 is regulated through DNA methylation. For the purpose, it analyzed data from the DNMIVD database to determine the degree of methylation of

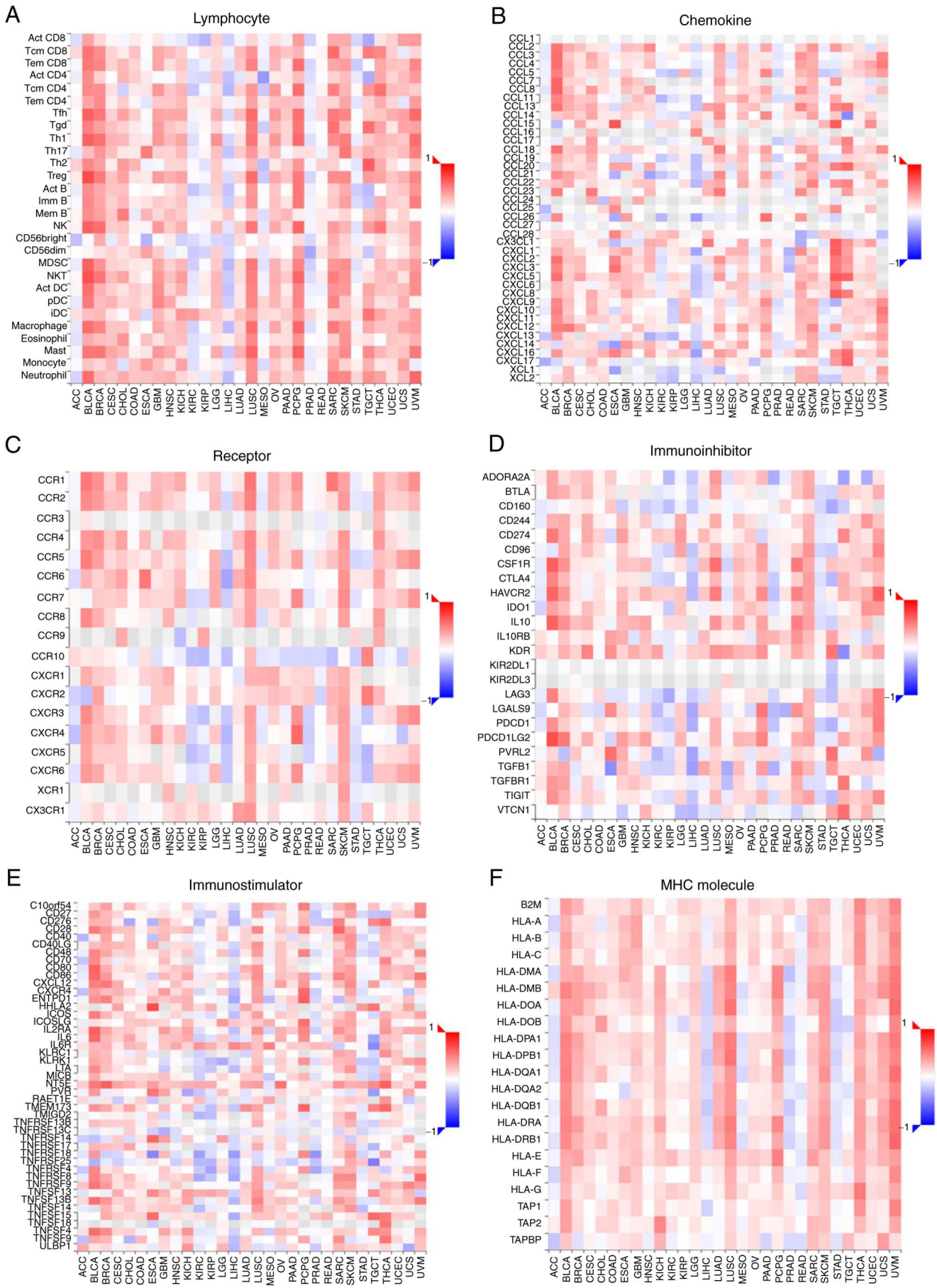

Figure 8. Correlations of DPP4 expressions with tumor-immune systems among different types of cancer. The correlations between DPP4 expression and (A) lymphocytes, (B) chemokine, (C) receptors, (D) immunosuppressants, (E) immunostimulants and (F) MHC molecules across pan-cancers. The Y axis indicates human immune molecules, whereas the X axis indicates human types of cancer. The full names of types of cancer are shown in Fig. 4.

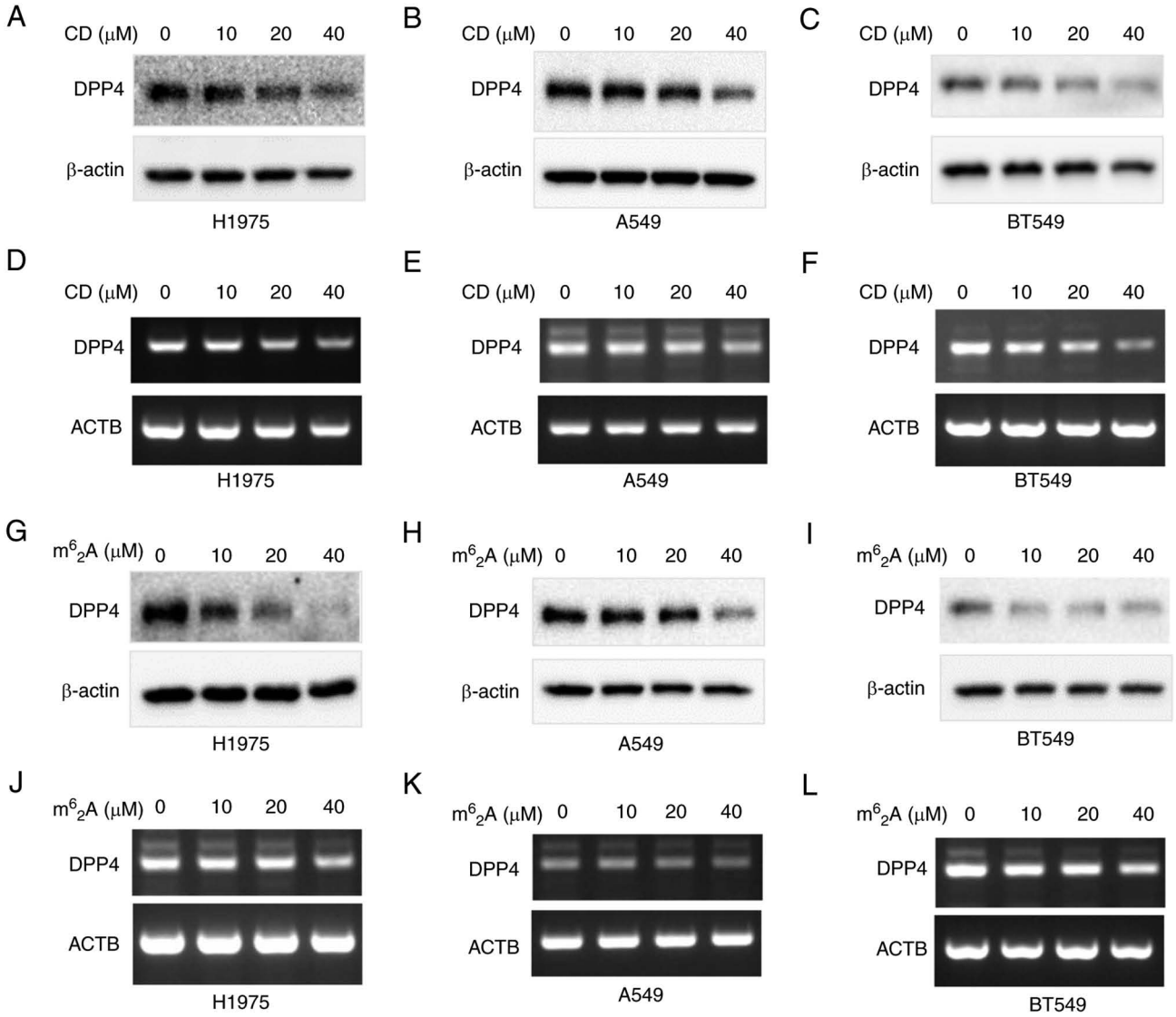

Figure 9. CD and $m^6{}_2A$ inhibit DPP4 expressions of both protein and mRNA in various cancer cells. CD decreases DPP4 expression in (A and D) H1975 lung cancer cells, (B and E) A549 lung cancer cells, (C and F) BT549 breast cancer cells. $m^6{}_2A$ decreases DPP4 expression in (G and J) H1975 lung cancer cells, (H and K) A549 lung cancer cells and (I and L) BT549 breast cancer cells. Panels A, B, C, G, H and I are protein expressions while panels D, E, F, J, K and L are mRNA expressions. CD, cordycepin; DPP4, dipeptidyl peptidase 4.

the *DPP4* promoter and changes in expression in 23 different types of cancer. It was found that the mRNA levels of *DPP4* were decreased in two types of cancer (BRCA and colon adenocarcinoma (COAD)) compared with matched healthy tissues; however DPP4 methylation levels were increased (Fig. 6A vs. B, E vs. F, respectively). The mRNA levels of *DPP4* were increased in THCA samples and the promoter regions of DPP4 were decreased in cancer tissues compared with matched healthy tissues (Fig. 6I vs. J). Pearson and Spearman correlation analyses showed the inverse correlations between promoter methylation and *DPP4* expression in BRCA, COAD and THCA compared with matched healthy tissues (Fig. 6C vs. D, G vs. H, K vs. L, respectively). However, P>0.05 in BRCA and COAD patients. Nevertheless, these results indicated that DNA methylation may be the mechanism regulating DPP4 expression in BRCA, COAD and THCA. Other mechanisms may be involved in the regulation of DPP4 expression in other types of cancer.

Altered DNA profiles of DPP4 in different types of cancer. It was recently reported that *DPP4* gene polymorphisms are associated with clinicopathological characteristics in oral cancer (67). The DPP4 rs3788979 polymorphism may be associated with severe COVID-19 (68). The present study analyzed the *DPP4* mutation profile in 32 different types of cancer to determine relationships with the development of malignancy, recurrence and therapeutic resistance. By analyzing *DPP4* mutations, it was found that uterine corpus endometrial carcinoma (UCEC) has the highest frequency of mutations (8.32% of 529 cases), followed by SKCM (4.95% of 444 cases); KIRC has the lowest frequency of mutations (0.39% of 511 cases; Fig. 7A). Fig. 7B shows structural variations, mutations, amplifications and deep deletions with mutations being the dominant type of alteration (Fig. 7A and B). There were no *DPP4* mutations found in the other seven types of cancer, which are presented in Fig. 7A. The detailed landscape included missense mutation, splicing, truncation and structural

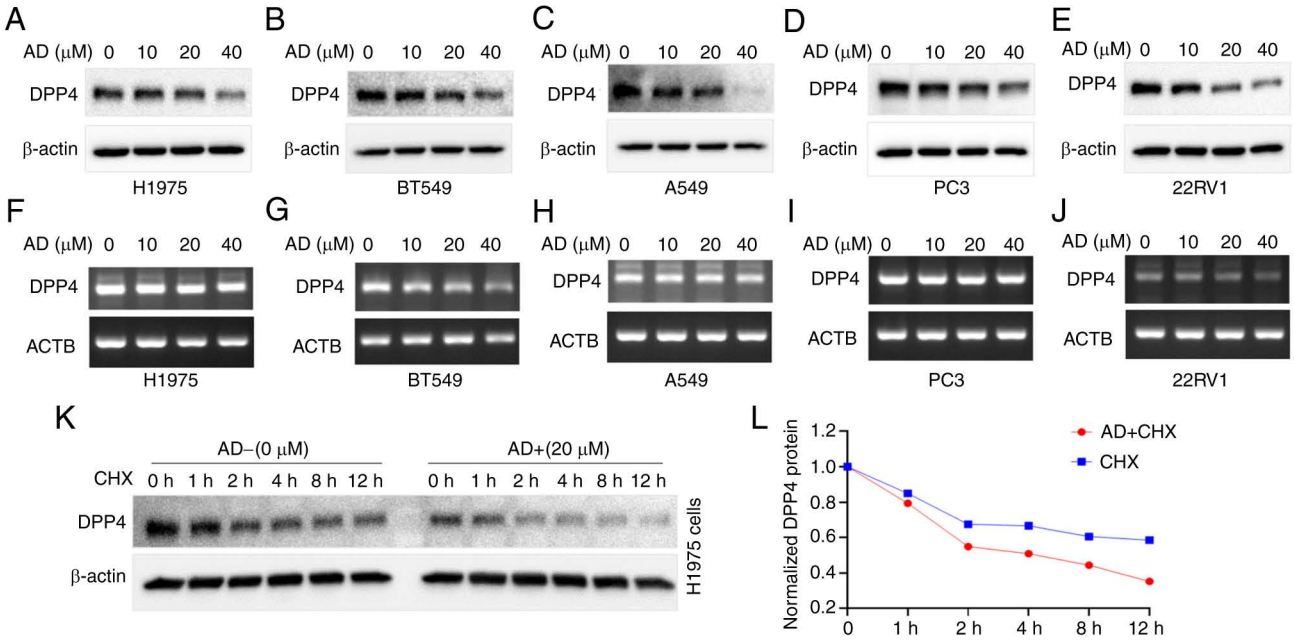

Figure 10. AD inhibits DPP4 expressions of both mRNA and protein in various types of cancer cells. AD regulates DPP4 expression in (A and F) H1975 lung cancer cell line, (B and G) BT549 breast cancer cell line and (C and H) A549 lung cancer cell line. (D and I) AD regulates DPP4 expression in the PC3 prostate cancer cell line. (E, J) AD regulates DPP4 expression in the 22RV1 prostate cancer cell line. (K) Treatment with AD promotes DPP4 protein degradation in H1975 cancer cells. The left panel shows without AD treatment, while the right panel shows AD treatment. (L) The quantitative results for Fig. 10K. The blue line shows CHX treatment only, while the red line shows CHX together with AD treatments. AD, adenosine; DPP4, dipeptidyl peptidase 4; CHX, cycloheximide.

variation/fusion along the whole *DPP4* gene, with missense mutation being the dominant type of alteration (Fig. 7C).

Association studies for DPP4 expression with tumor-immune systems in different types of cancer. The activity of DPP4 regulates numerous chemokines, cytokines and immunosuppressant/immunostimulants. DPP4 is also involved in cancer immunology (14). Immune system response plays indispensable roles in anti-viral and anti-cancer processes. Therefore, the present study conducted association studies to examine the relationship between *DPP4* mRNA expression and the extent of immune infiltration in different types of cancer. Notably, it found correlations between *DPP4* mRNA expression and immune lymphocytes (Fig. 8A), chemokines (Fig. 8B), receptors (Fig. 8C), immunosuppressants (Fig. 8D), immunostimulants (Fig. 8E) and major histocompatibility complex (MHC) molecules (Fig. 8F) in almost all types of cancer. These findings suggest therapeutic and preventive roles of DPP4 in cancer and SARS-CoV-2 invasion, respectively.

CD inhibits DPP4 expression in H1975, A549 and BT549 cancer cells. Small molecules or active substances derived from natural products can manipulate gene expression. The present study sought to determine whether these substances would target DPP4 expression. The effect of CD, a nucleoside derivative (adenosine derivative), on the expression of DPP4 was tested in a triple-negative breast cancer cell line (BT549) and two lung cancer cell lines (A549 and H1975). The results demonstrated that CD inhibited both DPP4 protein and mRNA expression in a dosage-dependent manner in H1975 (Fig. 9A and D), A549 (Fig. 9B and E) and BT549 (Fig. 9C and F) cells.

$m^6{}_2A$ inhibits DPP4 expression in H1975, A549 and BT549 cancer cells. The effect of $m^6{}_2A$, another adenosine derivative, on DPP4 expression was also tested in BT549, A549 and H1975 cells. The results indicated that $m^6{}_2A$ also inhibited both DPP4 protein and mRNA expression in a dosage-dependent manner in H1975 (Fig. 9G and J), A549 (Fig. 9H and K) and BT549 (Fig. 9I and L) cells.

The findings of the present study suggested that both the adenosine derivatives CD and $m^6{}_2A$ may have potential therapeutic value as anti-SARS-CoV-2 molecules through inhibition of DPP4 expression in cancer.

AD inhibits DPP4 expression in H1975, A549, BT549 and other cancer cells. The effect of AD on DPP4 expression was also investigated in H1975, A549, BT549 and other cancer cells. The results indicated that AD also inhibited DPP4 protein expression in a dosage-dependent manner in H1975 (Fig. 10A), BT549 (Fig. 10B) and A549 (Fig. 10C) cells. Moreover, we found that AD inhibited DPP4 protein expression in a dosage-dependent manner in the PC3 (Fig. 10D) and 22RV1 (Fig. 10E) prostate cancer cell line. Surprisingly, unlike CD and $m^6{}_2A$, AD did not induce significant changes in *DPP4* mRNA expression in these cell lines, except 22RV1 (Fig. 10F-J, respectively). Nevertheless, these results suggest that AD itself might exert therapeutic effects as an anti-SARS-CoV-2 agent through inhibition of DPP4 expression in cancer.

Based on the lack of change in the mRNA levels, the present study sought to investigate whether protein stability affects DPP4 protein expression. Thus, western blotting analysis was performed after CHX treatment with or without AD in H1975 cells. The results are shown in Fig. 10K, while the quantitated protein levels are shown in Fig. 10L. Treatment

Table I. Selected genes and their primer sequences for PCR.

Gene	Primers	Sequence (from 5'-3')	GenBank
IL6	RT-IL6-L	AGACAGCCACTCACCTCTTCA	NM_000600.5
	RT-IL6-R	TAAAGCTGCGCAGAATGAGAT	NM_000600.5
CD28	RT-CD28-L	TGTGAAAGGGAAACACCTTTG	NM_006139.4
	RT-CD28-R	TGAGATGTGCAGGTGAGTGAG	NM_006139.4
CD80	RT-CD80-L	CACCCTCCAATCTCTGTGTGT	NM_005191.4
	RT-CD80-R	TCCCCAGACATCATAGTCAGC	NM_005191.4
CD86	RT-CD86-L	GGGTGAAAGCTTTGCTTCTCT	NM_175862.4
	RT-CD86-R	GTCCAACTGTCCGAATCAAAA	NM_175862.4
IL10	RT-IL10-L	GAGTCCTTGCTGGAGGACTTT	NM_000572.3
	RT-IL10-R	GATGCCTTTCTCTTGGAGCTT	NM_000572.3
CTLA-4	RT-CTLA-4-L	CAACCTACATGATGGGGAATG	NM_005214.5
	RT-CTLA-4-R	TGCTTTTCACATTCTGGCTCT	NM_005214.5
LAG-3	RT-LAG-3-L	CAGAGATGGCTTCAACGTCTC	NM_002286.6
	RT-LAG-3-R	CTGGCTCACATCCTCTAGTCG	NM_002286.6
CXCL1	RT-CXCL1-L	CCCAAGAACATCCAAAGTGTG	NM_001511.4
	RT-CXCL1-R	CCTCTGCAGCTGTGTCTCTCT	NM_001511.4
CXCL2	RT-CXCL2-L	GGAATTCACCTCAAGAACATCC	NM_002089.4
	RT-CXCL2-R	CCTCTGCAGCTGTGTCTCTCT	NM_002089.4
CXCL3	RT-CXCL3-L	TGGGAAGAAAGCTTGTCTCAA	NM_002090.3
	RT-CXCL3-R	GTTCCCCACCCTGTCATTTAT	NM_002090.3
CXCL5	RT-CXCL5-L	AATCTTCGCTCCTCCAATCTC	NM_002994.5
	RT-CXCL5-R	CAAATTTCCTTCCCGTTCTTC	NM_002994.5
CXCL6	RT-CXCL6-L	ACCCCAAAACGATTGGTAAAC	NM_002993.4
	RT-CXCL6-R	TCTTACTGGGTCCAGGGATCT	NM_002993.4
CXCL8	RT-CXCL8-L	TTTGCCAAGGAGTGCTAAAGA	NM_000584.4
	RT-CXCL8-R	TATTGCATCTGGCAACCCTAC	NM_000584.4
A2AR	RT-A2AR-L	TCAACAGCAACCTGCAGAAC	NM_000675.6
	RT-A2AR-R	TCCAACCTAGCATGGGAGTC	NM_000675.6

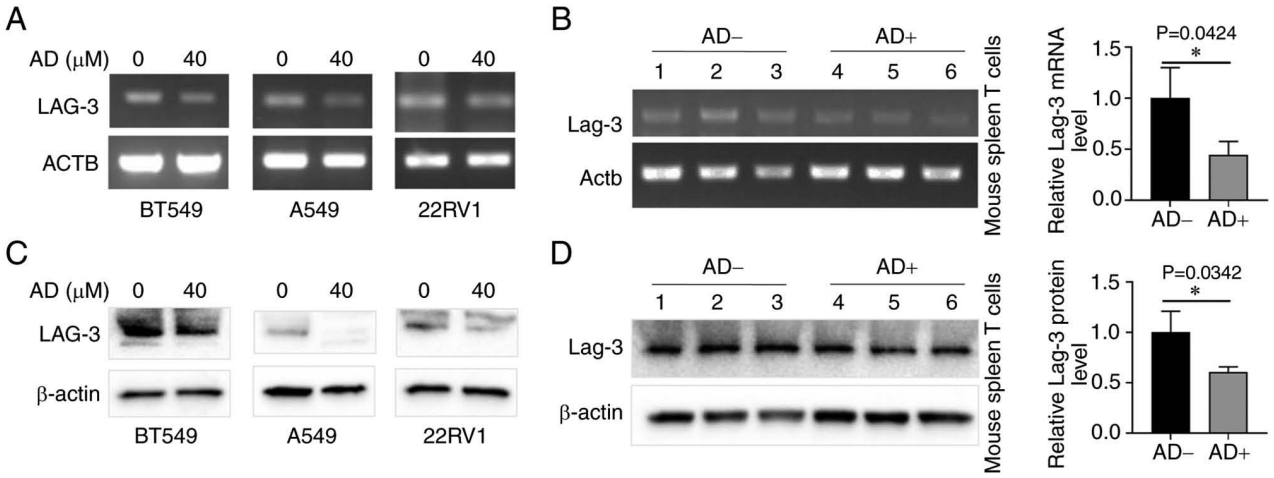

Figure 11. AD inhibits Lag-3 mRNA expressions *in vitro* and *in vivo*. (A and C) AD inhibits Lag-3 in (A) mRNA and (C) protein expressions in cancer cell lines of BT549 (left panel), A549 (middle panel) and 22RV1 (right panel). AD inhibits Lag-3 in (B) mRNA and (D) protein expressions in mice. Quantitative data were showed in the right panels. In Fig. 11B, AD inhibited the expression level of Lag-3 mRNA (P=0.0424) and in Fig. 11D, AD inhibited the expression level of Lag-3 protein (P=0.0342). *P<0.05 was considered statistically significant. AD, adenosine; Lag-3, lymphocyte activating 3.

with AD decreased the protein stability of DPP4 compared with control; the half-life of the protein was decreased from >12 h to ~4 h (Fig. 10K and L). These results indicate that treatment with AD could decrease the stability of DPP4 protein.

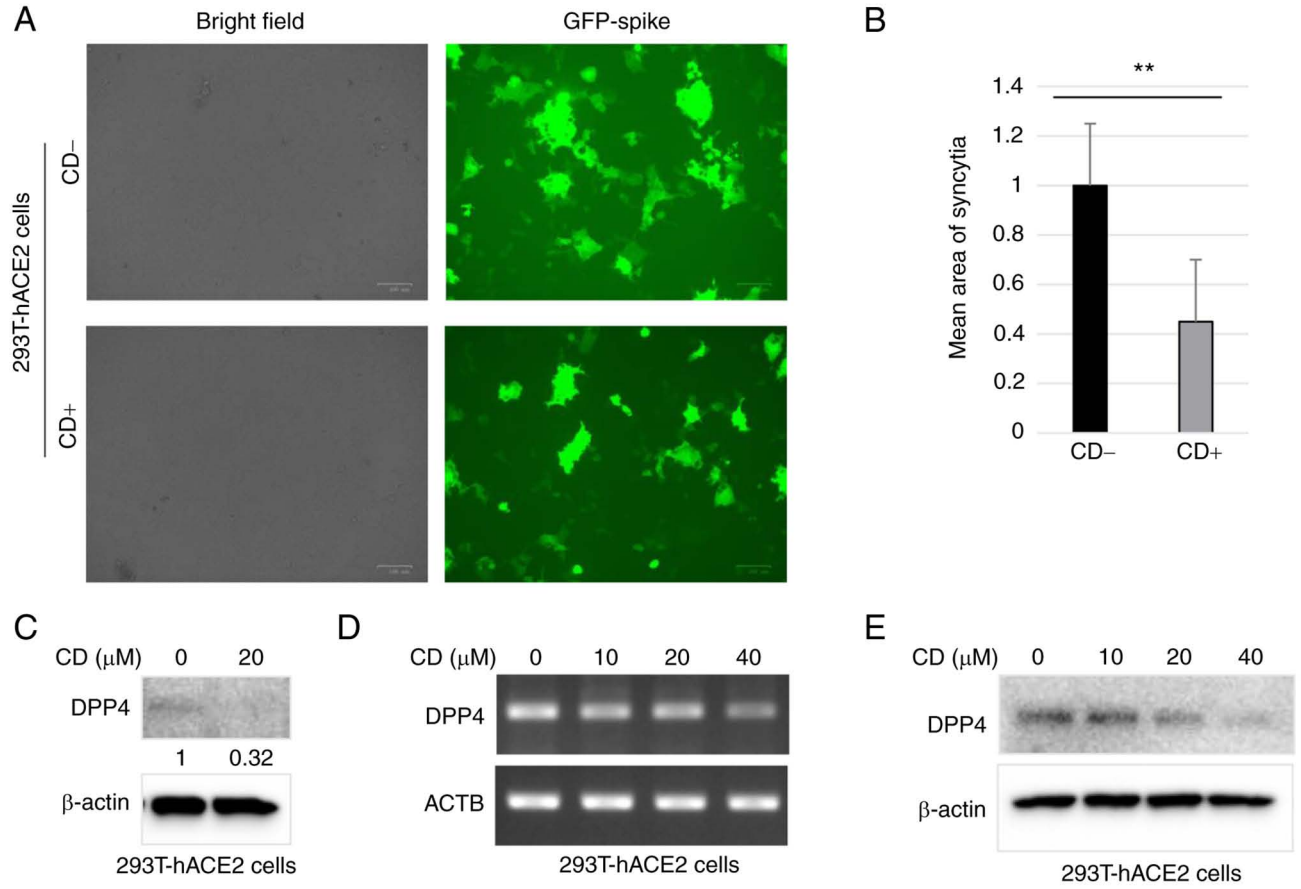

Figure 12. CD significantly inhibits syncytial formation. (A) Representative images of syncytia formation in control (CD-) and CD-treated (CD+) 293T-hACE2 cells. Magnification, x40. (B) The quantitative results of (A) (C) DPP4 protein levels in control (CD-) and CD-treated (CD+) 293T-hACE2 cells. DPP4 (D) mRNA and (E) protein levels in 293T-hACE2 cells with different amounts of CD treatment. Unpaired student test was used for statistical analysis. **P<0.01. CD, cordycepin; DPP4, dipeptidyl peptidase 4.

Role of AD in immune molecules and DPP4 expression associated genes. The TISIDB database analysis revealed that DPP4 regulates chemokines, cytokines and immunosuppressants/immunostimulants; the involvement of immune molecules from AD/A2AR signaling has been reported in the literature (69-72). The present study investigated which immune molecules are affected by AD and are associated with DPP4 expression. Cancer cell lines were treated with or without AD and semi-quantitative RT-PCR was conducted to examine the expression of 14 candidate genes (Table I). The results are shown in Fig. 11; AD downregulated the expression of LAG-3 in BT549, A549 and 22RV1 cells at both the mRNA (Fig. 11A) and protein (Fig. 11C) levels; however, it did not alter the levels of the other 13 genes (data not shown).

CD inhibits syncytial formation likely through DPP4. Evidence indicates that a large number of multinucleated cells characteristic of syncytial pathology are present in patients with COVID-19 (73). This is a pathological hallmark of SARS-CoV-2 infection. Syncytium formation is required for the participation of SARS-CoV-2 Spike protein and host cell having the human *ACE2* gene (62). In the present study, after treatment with CD, 293T-hACE2 cells were transfected with SARS-CoV-2-Spike plasmids with GFP fluorescence. Numerous large syncytia with GFP green fluorescence were observed in control cells, indicating SARS-CoV-2 cell invasion (Fig. 12A; upper panels). Notably, treatment with CD significantly decreased the area of fluorescence of GFP-positive syncytia (Fig. 12A; bottom panels). The quantitative results are shown in Fig. 12B; treatment with CD significantly reduced the mean fluorescence area of syncytia compared with the control group. The present study also investigated whether treatment with CD reduced syncytia formation, at least partially, through DPP4. Western blotting revealed that the levels of DPP4 protein were significantly decreased in 293T-hACE2 cells following treatment with CD compared with control (Fig. 12C). As expected, CD inhibited DPP4 expression in 293T-hACE2 cells at both the protein and mRNA levels in a dosage-dependent manner (Fig. 12D and E). Thus, CD may inhibit the formation of syncytia through DPP4.

Discussion

The present study found that, in healthy tissues, DPP4 was mainly expressed in in endocrine tissues, the gastrointestinal tract, female tissue (mainly in placenta), male tissue (mainly in prostate and seminal vesicle), proximal digestive tract, kidneys, bladder, liver, gallbladder and the respiratory system. Although the *DPP4* RNA levels were low (lung; 16.0 nTPM), the DPP4 protein expression was moderate, demonstrating its role in viral invasion in the lungs/bronchus/nasopharynx. Among

15 immune cell types, *DPP4* mRNA was mainly expressed in T cells (memory CD4 T-cell Th1/Th17). Compared with matched healthy tissues, the levels of *DPP4* were upregulated in ESCA, KIRP, LIHC, LUAD, PAAD, PRAD, STAD, THCA and THYM. In contrast, they were downregulated in BRCA, KICH, LUSC and SKCM. These findings indicated the roles of DPP4 in viral invasion in most types of cancer. Higher expression levels were associated with a long OS in KIRC and MESO, implying that DPP4 could be a favorable marker. However, high expression was also linked to a short OS in BLCA, LGG, LUSC, PRAD and UVM, suggesting that DPP4 could be an unfavorable marker. The isoform DPP4-001 includes both the DPPIV_N domain and Peptidase_S9 domain with 766 amino acids, indicating its function in tumorigenesis and SARS-CoV-2 invasion in patients with different types of cancer. DNA methylation in BRCA, COAD and THCA may be the mechanism regulating DPP4 expression. UCEC had the highest mutation frequency (8.32%), followed by SKCM (4.95%); KIRC had the lowest mutation frequency (0.39%). *DPP4* expression in tumor-immune systems revealed correlations between *DPP4* expression and immune lymphocytes, receptors, chemokines, immunosuppressants, immunostimulants and MHC molecules in almost all types of cancer. These results suggested a therapeutic role of DPP4 in cancer and SARS-CoV-2. The levels of soluble DPP4 (sDPP4) levels were increased in patients with acute and chronic viral infections; thus, the concentration of sDPP4 might be useful as a biomarker for these diseases (74). DPP4 inhibitors (e.g., gliptins) could be beneficial for patients with COVID-19, probably through interference with viral invasion (74) and activation of inflammatory pathways (75).

CD is a natural active substance derived from the traditional Chinese medicine fungus *Cordyceps militaris*, which possesses anticancer activity (76-78). $m^6{}_2A$ is a modified ribonucleoside in tRNA derived from *Mycobacterium bovis* Bacille Calmette-Guérin (79). CD and $m^6{}_2A$ are both derivatives of AD that suppress cathepsin L (CTSL) expression in cancer cells. CTSL is another receptor for SARS-CoV-2 (57). Additionally, CD suppresses the expression of other SARS-CoV-2 receptors (e.g., FURIN and transmembrane serine protease 2), in different cancer cells (47,80). Evidence indicates that a large number of multinucleated cells characteristic of syncytial pathology are present in patients with COVID-19 (73). This is a pathological hallmark of SARS-CoV-2 infection (62). Syncytium formation is required for the participation of SARS-CoV-2 Spike protein and host cell having human the *ACE2* gene (62). The present study demonstrated that CD inhibits syncytia formation likely through DPP4. As expected, CD and $m^6{}_2A$ inhibit DPP4 expression in cancer cells, suggesting anti-SARS-CoV-2 and anti-cancer role through suppression of DPP4 expression.

AD is regarded as a mainly metabolic and immune checkpoint regulator in the tumor microenvironment, implicated in tumor escape from the host immune system (81). Targeting the AD pathway could be useful for cancer immunotherapy (82,83). Markedly, AD inhibited DPP4 expression in five types of cancer cells; this suggested its therapeutic potential as an anti-SARS-CoV-2 agent by inhibiting DPP4 expression in cancer.

LAG-3 belongs to a novel class of immune checkpoint receptors. It is highly expressed in TILs of various solid tumors, such as colon cancer, hepatocellular carcinoma, head and neck cancer, non-small cell lung cancer and pancreatic cancer. In pathological states, LAG-3 is highly expressed at the TILs surfaces, which positively correlates with the development and occurrence of cancer (84). Similar to programmed cell death protein 1 (PD-1) and cytotoxic T-lymphocyte antigen 4, LAG-3 is considered a vital next-generation immune checkpoint molecule (85). Numerous LAG-3 inhibitors have been reported in 108 clinical trials (https://clinicaltrials.gov/) (86). Encouragingly, the first anti-LAG-3 inhibitor (monoclonal antibody), relatlimab (also called BMS-986016), has been approved for clinical use by the U.S. FDA. Moreover, in March 2022, relatlimab in combination with nivolumab (PD-1 inhibitor) was approved by the U.S. FDA under the name opdualag. This is the first antibody approved for the treatment of adult and pediatric patients with unresectable or metastatic melanoma. This therapeutic regimen triggered synergistic immune responses to increase the progression-free survival and reduce the number of unresponsive patients. Nivolumab is an important anti-PD-1 antibody for the treatment of different types of cancer (87,88); it has been approved for clinical use in more than 65 countries, including the USA and China (87). By analyzing the predicted genes for both DPP4 regulation and AD/A2AR signaling (69-72), the present study showed that AD downregulated LAG-3 expression in cancer cell lines, thereby demonstrating the anti-cancer synergistic effects of DPP4 and AD regulation. However, further research is warranted to elucidate the mechanism underlying DPP4 regulation and SARS-CoV-2 infection.

The present study showed that CD can inhibit viral entry by pseudovirus-SARS-CoV-2 (Spike protein) experiments shown in Fig. 12. Mouse experiments involving AD treatments followed western blotting and RT-PCR, showed in Fig. 11B and D. The two may demonstrate the anti-SARS-CoV-2 or immune response. However, the present study does not have data to show directly anti-cancer effect *in vitro* and *in vivo*. This is a limitation which may be addressed in the near future.

In conclusion, the present study revealed the importance of DPP4 in different types of cancer, susceptibility to SARS-CoV-2 attack and possible DPP4/AD/LAG-3 signaling. These data also indicated potential immunotherapy options for SARS-CoV-2 by targeting DPP4 using small molecules derived from natural products, such as $m^6{}_2A$, CD and AD. Further mechanism of DPP4 regulation and SARS-CoV-2 infection by these small molecules needs to be clarified in more detail.

Acknowledgments

The authors thank Dr Kai Wang and Mrs. Jiayue He from the Research Center for Preclinical Medicine, Southwest Medical University for their help in the syncytial formation experiment.

Funding

The present study was supported by the Foundation of Science and Technology Department of Sichuan Province (grant no. 2022NSFSC0737), the Joint Innovation Special Project of Science and Technology Plan of Sichuan Province (grant no. 2022YFS0623-C3), in part by the Research Foundation of Luzhou City (grant no. 2021-SYF-37)

and the National Natural Science Foundation of China (grant nos. 81672887, 82073263).

Availability of data and materials

All data generated or analyzed during this study are included in this published article.

Authors' contributions

JD, JiF, WZ, LZ and JC performed experimental studies, data acquisition, data analysis and sample collection. JuF and HC designed the project and analyzed the data. JuF and TH and supervised the project. JuF wrote and edited the manuscript. JD and JuF confirm the authenticity of all the raw data. All authors read and approved the final manuscript.

Ethics approval and consent to participate

The present study was reviewed and approved by the Ethics Committee of Southwest Medical University, Sichuan, China (approval no. 20221117-049). Informed consent was obtained from patients for tissues samples.

Patient consent for publication

Not applicable

Competing interests

The authors declare that they have no competing interests.

References

1. Daddona PE and Kelley WN: Human adenosine deaminase. Stoichiometry of the adenosine deaminase-binding protein complex. Biochim Biophys Acta 580: 302-311, 1979.
2. Kameoka J, Tanaka T, Nojima Y, Schlossman SF and Morimoto C: Direct association of adenosine deaminase with a T cell activation antigen, CD26. Science 261: 466-469, 1993.
3. Morrison ME, Vijayasaradhi S, Engelstein D, Albino AP and Houghton AN: A marker for neoplastic progression of human melanocytes is a cell surface ectopeptidase. J Exp Med 177: 1135-1143, 1993.
4. Abbott CA, Baker E, Sutherland GR and McCaughan GW: Genomic organization, exact localization, and tissue expression of the human CD26 (dipeptidyl peptidase IV) gene. Immunogenetics 40: 331-338, 1994.
5. Marguet D, Baggio L, Kobayashi T, Bernard AM, Pierres M, Nielsen PF, Ribel U, Watanabe T, Drucker DJ and Wagtmann N: Enhanced insulin secretion and improved glucose tolerance in mice lacking CD26. Proc Natl Acad Sci USA 97: 6874-6879, 2000.
6. Conarello SL, Li Z, Ronan J, Roy RS, Zhu L, Jiang G, Liu F, Woods J, Zycband E, Moller DE, *et al*: Mice lacking dipeptidyl peptidase IV are protected against obesity and insulin resistance. Proc Natl Acad Sci USA 100: 6825-6830, 2003.
7. Klemann C, Wagner L, Stephan M and von Horsten S: Cut to the chase: A review of CD26/dipeptidyl peptidase-4's (DPP4) entanglement in the immune system. Clin Exp Immunol 185: 1-21, 2016.
8. Vankadari N and Wilce JA: Emerging WuHan (COVID-19) coronavirus: Glycan shield and structure prediction of spike glycoprotein and its interaction with human CD26. Emerg Microbes Infect 9: 601-604, 2020.
9. Ohnuma K, Uchiyama M, Yamochi T, Nishibashi K, Hosono O, Takahashi N, Kina S, Tanaka H, Lin X, Dang NH and Morimoto C: Caveolin-1 triggers T-cell activation via CD26 in association with CARMA1. J Biol Chem 282: 10117-10131, 2007.
10. Gines S, Marino M, Mallol J, Canela EI, Morimoto C, Callebaut C, Hovanessian A, Casadó V, Lluis C and Franco R: Regulation of epithelial and lymphocyte cell adhesion by adenosine deaminase-CD26 interaction. Biochem J 361: 203-209, 2002.
11. Ohnuma K, Hatano R, Komiya E, Otsuka H, Itoh T, Iwao N, Kaneko Y, Yamada T, Dang NH and Morimoto C: A novel role for CD26/dipeptidyl peptidase IV as a therapeutic target. Front Biosci (Landmark Ed) 23: 1754-1779, 2018.
12. Zhang T, Tong X, Zhang S, Wang D, Wang L, Wang Q and Fan H: The roles of dipeptidyl peptidase 4 (DPP4) and DPP4 inhibitors in different lung diseases: New evidence. Front Pharmacol 12: 731453, 2021.
13. da Cruz Freire JE, Junior JEM, Pinheiro DP, da Cruz Paiva Lima GE, do Amaral CL, Veras VR, Madeira MP, Freire EBL, Ozório RG, Fernandes VO, *et al*: Evaluation of the anti-diabetic drug sitagliptin as a novel attenuate to SARS-CoV-2 evidence-based in silico: Molecular docking and molecular dynamics. 3 Biotech 12: 344, 2022.
14. Scheen AJ: Cardiovascular effects of dipeptidyl peptidase-4 inhibitors: From risk factors to clinical outcomes. Postgrad Med 125: 7-20, 2013.
15. Hu X, Wang X and Xue X: Therapeutic perspectives of CD26 inhibitors in imune-mediated diseases. Molecules 27: 4498, 2022.
16. Thompson MA, Ohnuma K, Abe M, Morimoto C and Dang NH: CD26/dipeptidyl peptidase IV as a novel therapeutic target for cancer and immune disorders. Mini Rev Med Chem 7: 253-273, 2007.
17. Alkharsah KR, Aljaroodi SA, Rahman JU, Alnafie AN, Al Dossary R, Aljindan RY, Alnimr AM and Hussen J: Low levels of soluble DPP4 among Saudis may have constituted a risk factor for MERS endemicity. PLoS One 17: e0266603, 2022.
18. Wang N, Shi X, Jiang L, Zhang S, Wang D, Tong P, Guo D, Fu L, Cui Y, Liu X, *et al*: Structure of MERS-CoV spike receptor-binding domain complexed with human receptor DPP4. Cell Res 23: 986-993, 2013.
19. Sedo A, Krepela E, Kasafirek E, Kraml J and Kadlecova L: Dipeptidyl peptidase IV in the human lung and spinocellular lung cancer. Physiol Res 40: 359-362, 1991.
20. Bishnoi R, Hong YR, Shah C, Ali A, Skelton WP IV, Huo J, Dang NH and Dang LH: Dipeptidyl peptidase 4 inhibitors as novel agents in improving survival in diabetic patients with colorectal cancer and lung cancer: A surveillance epidemiology and endpoint research medicare study. Cancer Med 8: 3918-3927, 2019.
21. Colice G, Price D, Gerhardsson de Verdier M, Rabon-Stith K, Ambrose C, Cappell K, Irwin DE, Juneau P and Vlahiotis A: The effect of DPP-4 inhibitors on asthma control: An administrative database study to evaluate a potential pathophysiological relationship. Pragmat Obs Res 8: 231-240, 2017.
22. Raj VS, Smits SL, Provacia LB, van den Brand JM, Wiersma L, Ouwendijk WJ, Bestebroer TM, Spronken MI, van Amerongen G, Rottier PJ, *et al*: Adenosine deaminase acts as a natural antagonist for dipeptidyl peptidase 4-mediated entry of the Middle East respiratory syndrome coronavirus. J Virol 88: 1834-1838, 2014.
23. deKay JT, May TL, Riker RR, Rud J, Gagnon DJ, Sawyer DB, Seder DB and Ryzhov S: The number of circulating CD26 expressing cells is decreased in critical COVID-19 illness. Cytometry A: Mar 16, 2022 (Epub ahead of print).
24. Cameron K, Rozano L, Falasca M and Mancera RL: Does the SARS-CoV-2 spike protein receptor binding domain interact effectively with the DPP4 (CD26) Receptor? A Molecular Docking Study. Int J Mol Sci 22: 7001, 2021.
25. Govender Y, Shalekoff S, Ebrahim O, Waja Z, Chaisson RE, Martinson N and Tiemessen CT: Systemic DPP4/CD26 is associated with natural HIV-1 control: Implications for COVID-19 susceptibility. Clin Immunol 230: 108824, 2021.
26. Nadasdi A, Sinkovits G, Bobek I, Lakatos B, Förhécz Z, Prohászka ZZ, Réti M, Arató M, Cseh G, Masszi T, *et al*: Decreased circulating dipeptidyl peptidase-4 enzyme activity is prognostic for severe outcomes in COVID-19 inpatients. Biomark Med 16: 317-330, 2022.
27. Radzikowska U, Ding M, Tan G, Zhakparov D, Peng Y, Wawrzyniak P, Wang M, Li S, Morita H, Altunbulakli C, *et al*: Distribution of ACE2, CD147, CD26, and other SARS-CoV-2 associated molecules in tissues and immune cells in health and in asthma, COPD, obesity, hypertension, and COVID-19 risk factors. Allergy 75: 2829-2845, 2020.

28. Kawasaki T, Chen W, Htwe YM, Tatsumi K and Dudek SM: DPP4 inhibition by sitagliptin attenuates LPS-induced lung injury in mice. Am J Physiol Lung Cell Mol Physiol 315: L834-L845, 2018.
29. Kifle ZD, Woldeyohanin AE and Demeke CA: SARS-CoV-2 and diabetes: A potential therapeutic effect of dipeptidyl peptidase 4 inhibitors in diabetic patients diagnosed with COVID-19. Metabol Open 12: 100134, 2021.
30. Nitulescu GM, Paunescu H, Moschos SA, Petrakis D, Nitulescu G, Ion GND, Spandidos DA, Nikolouzakis TK, Drakoulis N and Tsatsakis A: Comprehensive analysis of drugs to treat SARSCoV2 infection: Mechanistic insights into current COVID19 therapies (Review). Int J Mol Med 46: 467-488, 2020.
31. Gordon DE, Jang GM, Bouhaddou M, Xu J, Obernier K, White KM, O'Meara MJ, Rezelj VV, Guo JZ, Swaney DL, *et al*: A SARS-CoV-2 protein interaction map reveals targets for drug repurposing. Nature 583: 459-468, 2020.
32. Pal R, Banerjee M, Mukherjee S, Bhogal RS, Kaur A and Bhadada SK: Dipeptidyl peptidase-4 inhibitor use and mortality in COVID-19 patients with diabetes mellitus: An updated systematic review and meta-analysis. Ther Adv Endocrinol Metab 12: 2042018821996482, 2021.
33. Han T, Ma S, Sun C, Zhang H, Qu G, Chen Y, Cheng C, Chen EL, Ayaz Ahmed M, Kim KY, *et al*: Association between anti-diabetic agents and clinical outcomes of COVID-19 in patients with diabetes: A systematic review and meta-analysis. Arch Med Res 53: 186-195, 2022.
34. Zein A and Raffaello WM: Dipeptidyl peptidase-4 (DPP-IV) inhibitor was associated with mortality reduction in COVID-19-A systematic review and meta-analysis. Prim Care Diabetes 16: 162-167, 2022.
35. Rakhmat, II, Kusmala YY, Handayani DR, Juliastuti H, Nawangsih EN, Wibowo A, Lim MA and Pranata R: Dipeptidyl peptidase-4 (DPP-4) inhibitor and mortality in coronavirus disease 2019 (COVID-19)-A systematic review, meta-analysis, and meta-regression. Diabetes Metab Syndr 15: 777-782, 2021.
36. Carrasco-Sanchez FJ, Carretero-Anibarro E, Gargallo MÁ, Gómez-Huelgas R, Merino-Torres JF, Orozco-Beltrán D, Pines Corrales PJ and Ruiz Quintero MA: Executive Summary from Expert consensus on effectiveness and safety of iDPP-4 in the treatment of patients with diabetes and COVID-19. Endocrinol Diabetes Nutr (Engl Ed) 69: 209-218, 2022.
37. Shestakova MV, Vikulova OK, Elfimova AR, Deviatkin AA, Dedov II and Mokrysheva NG: Risk factors for COVID-19 case fatality rate in people with type 1 and type 2 diabetes mellitus: A nationwide retrospective cohort study of 235,248 patients in the Russian Federation. Front Endocrinol (Lausanne) 13: 909874, 2022.
38. Solerte SB, Di Sabatino A, Galli M and Fiorina P: Dipeptidyl peptidase-4 (DPP4) inhibition in COVID-19. Acta Diabetol 57: 779-783, 2020.
39. Sebastian-Martin A, Sanchez BG, Mora-Rodriguez JM, Bort A and Diaz-Laviada I: Role of dipeptidyl Peptidase-4 (DPP4) on COVID-19 physiopathology. Biomedicines 10: 2026, 2022.
40. Ojha R, Gurjar K, Ratnakar TS, Mishra A and Prajapati VK: Designing of a bispecific antibody against SARS-CoV-2 spike glycoprotein targeting human entry receptors DPP4 and ACE2. Hum Immunol 83: 346-355, 2022.
41. Elkrief A, Hennessy C, Kuderer NM, Rubinstein SM, Wulff-Burchfield E, Rosovsky RP, Vega-Luna K, Thompson MA, Panagiotou OA, Desai A, *et al*: Geriatric risk factors for serious COVID-19 outcomes among older adults with cancer: A cohort study from the COVID-19 and Cancer Consortium. Lancet Healthy Longev 3: e143-e152, 2022.
42. Desai A, Gupta R, Advani S, Ouellette L, Kuderer NM, Lyman GH and Li A: Mortality in hospitalized patients with cancer and coronavirus disease 2019: A systematic review and meta-analysis of cohort studies. Cancer 127: 1459-1468, 2021.
43. Grivas P, Khaki AR, Wise-Draper TM, French B, Hennessy C, Hsu CY, Shyr Y, Li X, Choueiri TK, Painter CA, *et al*: Association of clinical factors and recent anticancer therapy with COVID-19 severity among patients with cancer: A report from the COVID-19 and Cancer Consortium. Ann Oncol 32: 787-800, 2021.
44. Fu C, Stoeckle JH, Masri L, Pandey A, Cao M, Littman D, Rybstein M, Saith SE, Yarta K, Rohatgi A, *et al*: COVID-19 outcomes in hospitalized patients with active cancer: Experiences from a major New York City health care system. Cancer 127: 3466-3475, 2021.
45. Beckenkamp A, Davies S, Willig JB and Buffon A: DPPIV/CD26: A tumor suppressor or a marker of malignancy? Tumour Biol 37: 7059-7073, 2016.
46. Fu J, Liao L, Balaji KS, Wei C, Kim J and Peng J: Epigenetic modification and a role for the E3 ligase RNF40 in cancer development and metastasis. Oncogene 40: 465-474, 2021.
47. Li D, Liu X, Zhang L, He J, Chen X, Liu S, Fu J, Fu S, Chen H, Fu J and Cheng J: COVID-19 disease and malignant cancers: The impact for the furin gene expression in susceptibility to SARS-CoV-2. Int J Biol Sci 17: 3954-3967, 2021.
48. Uhlen M, Fagerberg L, Hallstrom BM, Lindskog C, Oksvold P, Mardinoglu A, Sivertsson Å, Kampf C, Sjöstedt E, Asplund A, *et al*: Proteomics. Tissue-based map of the human proteome. Science 347: 1260419, 2015.
49. Uhlen M, Zhang C, Lee S, Sjöstedt E, Fagerberg L, Bidkhori G, Benfeitas R, Arif M, Liu Z, Edfors F, *et al*: A pathology atlas of the human cancer transcriptome. Science 357: eaan2507, 2017.
50. Tang Z, Li C, Kang B, Gao G, Li C and Zhang Z: GEPIA: A web server for cancer and normal gene expression profiling and interactive analyses. Nucleic Acids Res 45: W98-W102, 2017.
51. Tang Z, Kang B, Li C, Chen T and Zhang Z: GEPIA2: An enhanced web server for large-scale expression profiling and interactive analysis. Nucleic Acids Res 47: W556-W560, 2019.
52. Ding W, Chen J, Feng G, Chen G, Wu J, Guo Y, Ni X and Shi T: DNMIVD: DNA methylation interactive visualization database. Nucleic Acids Res 48: D856-D862, 2020.
53. Cerami E, Gao J, Dogrusoz U, Gross BE, Sumer SO, Aksoy BA, Jacobsen A, Byrne CJ, Heuer ML, Larsson E, *et al*: The cBio cancer genomics portal: An open platform for exploring multidimensional cancer genomics data. Cancer Discov 2: 401-404, 2012.
54. Ru B, Wong CN, Tong Y, Zhong JY, Zhong SSW, Wu WC, Chu KC, Wong CY, Lau CY, Chen I, *et al*: TISIDB: An integrated repository portal for tumor-immune system interactions. Bioinformatics 35: 4200-4202, 2019.
55. Fu J, Li L and Lu G: Relationship between microdeletion on Y chromosome and patients with idiopathic azoospermia and severe oligozoospermia in the Chinese. Chin Med J (Engl) 115: 72-75, 2002.
56. Zhang L, Yang M, Gan L, He T, Xiao X, Stewart MD, Liu X, Yang L, Zhang T, Zhao Y and Fu J: DLX4 upregulates TWIST and enhances tumor migration, invasion and metastasis. Int J Biol Sci 8: 1178-1187, 2012.
57. Zhang L, Wei C, Li D, He J, Liu S, Deng H, Cheng J, Du J, Liu X, Chen H, *et al*: COVID-19 receptor and malignant cancers: Association of CTSL expression with susceptibility to SARS-CoV-2. Int J Biol Sci 18: 2362-2371, 2022.
58. Wang K, Deng H, Song B, He J, Liu S, Fu J, Zhang L, Li D, Balaji KS, Mei Z, *et al*: The correlation between immune invasion and SARS-COV-2 entry protein ADAM17 in cancer patients by bioinformatic analysis. Front Immunol 13: 923516, 2022.
59. Wei C, Liu Y, Liu X, Cheng J, Fu J, Xiao X, Moses RE, Li X and Fu J: The speckle-type POZ protein (SPOP) inhibits breast cancer malignancy by destabilizing TWIST1. Cell Death Discov 8: 389, 2022.
60. Fu J, Song B, Du J, Liu S, He J, Xiao T, Zhou B, Li D, Liu X, He T, *et al*: Impact of BSG/CD147 gene expression on diagnostic, prognostic and therapeutic strategies towards malignant cancers and possible susceptibility to SARS-CoV-2. Mol Biol Rep: 1-13, 2022 doi: 10.1007/s11033-022-08231-1 (Epub ahead of print).
61. Liu G, Du W, Sang X, Tong Q, Wang Y, Chen G, Yuan Y, Jiang L, Cheng W, Liu D, *et al*: RNA G-quadruplex in TMPRSS2 reduces SARS-CoV-2 infection. Nat Commun 13: 1444, 2022.
62. Jocher G, Grass V, Tschirner SK, Riepler L, Breimann S, Kaya T, Oelsner M, Hamad MS, Hofmann LI, Blobel CP, *et al*: ADAM10 and ADAM17 promote SARS-CoV-2 cell entry and spike protein-mediated lung cell fusion. EMBO Rep 23: e54305, 2022.
63. Fu J, Zhou B, Zhang L, Balaji KS, Wei C, Liu X, Chen H, Peng J and Fu J: Expressions and significances of the angiotensin-converting enzyme 2 gene, the receptor of SARS-CoV-2 for COVID-19. Mol Biol Rep 47: 4383-4392, 2020.
64. Győrffy B, Lanczky A, Eklund AC, Denkert C, Budczies J, Li Q and Szallasi Z: An online survival analysis tool to rapidly assess the effect of 22,277 genes on breast cancer prognosis using microarray data of 1,809 patients. Breast Cancer Res Treat 123: 725-731, 2010.
65. Blume C, Jackson CL, Spalluto CM, Legebeke J, Nazlamova L, Conforti F, Perotin JM, Frank M, Butler J, Crispin M, *et al*: A novel ACE2 isoform is expressed in human respiratory epithelia and is upregulated in response to interferons and RNA respiratory virus infection. Nat Genet 53: 205-214, 2021.

66. Onabajo OO, Banday AR, Stanifer ML, Yan W, Obajemu A, Santer DM, Florez-Vargas O, Piontkivska H, Vargas JM, Ring TJ, *et al*: Interferons and viruses induce a novel truncated ACE2 isoform and not the full-length SARS-CoV-2 receptor. Nat Genet 52: 1283-1293, 2020.
67. Chen PJ, Lu HJ, Nassef Y, Lin CW, Chuang CY, Lee CY, Chiu YW, Yang SF and Yang WE: Association of dipeptidyl peptidase IV polymorphism with clinicopathological characters of oral cancer. J Oral Pathol Med 51: 730-737, 2022.
68. Posadas-Sanchez R, Sanchez-Munoz F, Guzman-Martin CA, Hernández-Díaz Couder A, Rojas-Velasco G, Fragoso JM and Vargas-Alarcón G: Dipeptidylpeptidase-4 levels and DPP4 gene polymorphisms in patients with COVID-19. Association with disease and with severity. Life Sci 276: 119410, 2021.
69. Cekic C and Linden J: Purinergic regulation of the immune system. Nat Rev Immunol 16: 177-192, 2016.
70. Fong L, Hotson A, Powderly JD, Sznol M, Heist RS, Choueiri TK, George S, Hughes BGM, Hellmann MD, Shepard DR, *et al*: Adenosine 2A receptor blockade as an immunotherapy for treatment-refractory renal cell cancer. Cancer Discov 10: 40-53, 2020.
71. Novitskiy SV, Ryzhov S, Zaynagetdinov R, Goldstein AE, Huang Y, Tikhomirov OY, Blackburn MR, Biaggioni I, Carbone DP, Feoktistov I and Dikov MM: Adenosine receptors in regulation of dendritic cell differentiation and function. Blood 112: 1822-1831, 2008.
72. Liu J, Shi Y, Liu X, Zhang D, Bai Y, Xu Y and Wang M: Blocking Adenosine/A2AR pathway for cancer therapy. Zhongguo Fei Ai Za Zhi 25: 460-467, 2022 (In Chinese).
73. Braga L, Ali H, Secco I, Chiavacci E, Neves G, Goldhill D, Penn R, Jimenez-Guardeño JM, Ortega-Prieto AM, Bussani R, *et al*: Drugs that inhibit TMEM16 proteins block SARS-CoV-2 spike-induced syncytia. Nature 594: 88-93, 2021.
74. Krejner-Bienias A, Grzela K and Grzela T: DPP4 inhibitors and COVID-19-holy grail or another dead end? Arch Immunol Ther Exp (Warsz) 69: 1, 2021.
75. Alomair BM, Al-Kuraishy HM, Al-Buhadily AK, Al-Gareeb AI, De Waard M, Elekhnawy E and Batiha GE: Is sitagliptin effective for SARS-CoV-2 infection: False or true prophecy? Inflammopharmacology 30: 2411-2415, 2022.
76. Radhi M, Ashraf S, Lawrence S, Tranholm AA, Wellham PAD, Hafeez A, Khamis AS, Thomas R, McWilliams D and de Moor CH: A systematic review of the biological effects of cordycepin. Molecules 26: 5886, 2021.
77. Tima S, Tapingkae T, To-Anun C, Noireung P, Intaparn P, Chaiyana W, Sirithunyalug J, Panyajai P, Viriyaadhammaa N, Nirachonkul W, *et al*: Antileukaemic cell proliferation and cytotoxic activity of edible golden cordyceps (*Cordyceps militaris*) extracts. Evid Based Complement Alternat Med 2022: 5347718, 2022.
78. Wei C, Khan MA, Du J, Cheng J, Tania M, Leung EL and Fu J: Cordycepin Inhibits triple-negative breast cancer cell migration and invasion by regulating EMT-TFs SLUG, TWIST1, SNAIL1, and ZEB1. Front Oncol 12: 898583, 2022.
79. Chan CT, Chionh YH, Ho CH, Lim KS, Babu IR, Ang E, Wenwei L, Alonso S and Dedon PC: Identification of N6,N6-dimethyladenosine in transfer RNA from Mycobacterium bovis Bacille Calmette-Guerin. Molecules 16: 5168-5181, 2011.
80. Fu J, Liu S, Tan Q, Liu Z, Qian J, Li T, Du J, Song B, Li D, Zhang L, *et al*: Impact of TMPRSS2 Expression, Mutation Prognostics, and Small Molecule (CD, AD, TQ, and TQFL12) Inhibition on Pan-Cancer Tumors and Susceptibility to SARS-CoV-2. Molecules 27: 7413, 2022.
81. Boison D and Yegutkin GG: Adenosine metabolism: Emerging concepts for cancer therapy. Cancer Cell 36: 582-596, 2019.
82. Hammami A, Allard D, Allard B and Stagg J: Targeting the adenosine pathway for cancer immunotherapy. Semin Immunol 42: 101304, 2019.
83. Vijayan D, Young A, Teng MWL and Smyth MJ: Targeting immunosuppressive adenosine in cancer. Nat Rev Cancer 17: 709-724, 2017.
84. Huo JL, Wang YT, Fu WJ, Lu N and Liu ZS: The promising immune checkpoint LAG-3 in cancer immunotherapy: From basic research to clinical application. Front Immunol 13: 956090, 2022.
85. Chocarro L, Blanco E, Zuazo M, Arasanz H, Bocanegra A, Fernández-Rubio L, Morente P, Fernández-Hinojal G, Echaide M, Garnica M, *et al*: Understanding LAG-3 Signaling. Int J Mol Sci 22: 5282, 2021.
86. Chocarro L, Bocanegra A, Blanco E, Fernández-Rubio L, Arasanz H, Echaide M, Garnica M, Ramos P, Piñeiro-Hermida S, Vera R, *et al*: Cutting-Edge: Preclinical and clinical development of the first approved Lag-3 inhibitor. Cells 11: 2351, 2022.
87. Robert C, Long GV, Brady B, Dutriaux C, Maio M, Mortier L, Hassel JC, Rutkowski P, McNeil C, Kalinka-Warzocha E, *et al*: Nivolumab in previously untreated melanoma without BRAF mutation. N Engl J Med 372: 320-330, 2015.
88. Ansell SM, Lesokhin AM, Borrello I, Halwani A, Scott EC, Gutierrez M, Schuster SJ, Millenson MM, Cattry D, Freeman GJ, *et al*: PD-1 blockade with nivolumab in relapsed or refractory Hodgkin's lymphoma. N Engl J Med 372: 311-319, 2015.

This work is licensed under a Creative Commons Attribution-NonCommercial-NoDerivatives 4.0 International (CC BY-NC-ND 4.0) License.